

1 Earliest infections predict the age distribution 2 of seasonal influenza A cases

3 Philip Arevalo¹, Huong Q. McLean², Edward A. Belongia², Sarah Cobey¹

4 For correspondence:

5 Philip Arevalo, parevalo@uchicago.edu

6 ¹Department of Ecology and Evolution, University of Chicago, Chicago, United States; ² Center for Clinical
7 Epidemiology and Population Health, Marshfield Clinic Research Institute, Marshfield, United States

8 Abstract

9 Seasonal variation in the age distribution of influenza A cases suggests that factors other than age shape susceptibility to
10 infection. We ask whether these differences can be explained in part by protection conferred by childhood influenza infection,
11 which has lasting impacts on immune responses to influenza and protection against novel influenza A subtypes (phenomena
12 known as original antigenic sin and immune imprinting). Fitting a statistical model to data from studies of influenza vaccine
13 effectiveness (VE), we find that primary infection appears to reduce the risk of medically attended infection with that subtype
14 throughout life. This effect is stronger for H1N1 compared to H3N2. Additionally, we find evidence that influenza VE varies
15 with both age and birth year, but not with the imprinting subtype, indicating that VE may be sensitive to particular exposure
16 histories. The ability to predict age-specific risk might improve forecasting models and vaccination strategies to combat
17 seasonal influenza.

18 Introduction

19 Seasonal influenza is a serious public health concern, resulting in over 100,000 hospitalizations and 4,000 deaths per year in
20 the United States despite extensive annual vaccination campaigns (Reed et al., 2015). The rapid evolution of the virus to
21 escape preexisting immunity contributes to the relatively high incidence of influenza, including in previously infected older
22 children and adults. How susceptibility arises and changes over time in the host population has been difficult to quantify.

23 A pathogen's rate of antigenic evolution should affect the mean age of the hosts it infects, and differences in the rate of
24 antigenic evolution have been proposed to explain differences in the age distributions of the two subtypes of influenza A.
25 Compared to H3N2, H1N1 disproportionately infects children (Caini et al., 2018; Khiabani et al., 2009). It also evolves
26 antigenically more slowly (Bedford et al., 2015). Thus, compared to H3N2, H1N1 is slower to escape immunity in individuals
27 who have experienced prior infection (namely older children and adults), making them less susceptible to reinfection (Bedford
28 et al., 2015; Beauté et al., 2015; Caini et al., 2018; Khiabani et al., 2009). H3N2, in contrast, exhibits well known changes
29 in antigenic phenotype that are expected to drive cases toward adults (Smith et al., 2004; Cobey and Koelle, 2008). Under this
30 simple model, hosts previously infected with a subtype face equal risk of reinfection (on challenge) with an antigenic variant
31 of that subtype.

32 The age distributions of influenza infections in exceptional circumstances—pandemics and spillovers of avian influenza—
33 have shown unexpected variation that suggests potentially complex effects of prior infection. Excess mortality in some adult
34 cohorts during the 1918 and 2009 H1N1 pandemics has been linked to childhood infection with particular subtypes (Gagnon
35 et al., 2013; Worobey et al., 2014; Gagnon et al., 2018). In the post-2009 pandemic period, excess mortality and hospitalization
36 in these cohorts was observed during H1N1-dominated seasons (Budd et al., 2019). Similarly, the subtypes circulating in
37 childhood predict individuals' susceptibility to severe zoonotic infections with avian H5N1 and H7N9, regardless of later
38 exposure to other seasonal subtypes (Gostic et al., 2016). These patterns suggest that early influenza infections, and not prior
39 infection per se, strongly shape susceptibility.

40 Early infections might also affect the protection conferred by influenza vaccination. Foundational work on the theory of
41 original antigenic sin demonstrated that an individual's immune response to influenza vaccination is biased toward antigens
42 similar to those encountered in childhood (Davenport and Hennessy, 1956, 1957). In some cases, this may result in an
43 extremely narrow antibody response focused on a single epitope (Davis et al., 2018). This phenomenon has been suggested

44 to explain an unexpected decrease in vaccine effectiveness (VE) in the middle-aged in the 2015-2016 influenza season
45 (Skowronski et al., 2017b; Flannery et al., 2018). More generally, it has been hypothesized that biases in immune memory can
46 arise from both past infections and vaccinations, leading to variation in vaccine effectiveness that is sensitive to the precise
47 history of exposures (Smith et al., 1999; Skowronski et al., 2017a).

48 To measure the effect of early exposures on infection risk and VE, we fitted statistical models to 3493 influenza cases
49 identified through seasonal studies of influenza VE from the 2007-2008 to 2017-2018 seasons in Marshfield, Wisconsin
50 (Belongia et al., 2009, 2011; Griffin et al., 2011; Treanor et al., 2012; Ohmit et al., 2014; McLean et al., 2014b; Gaglani et al.,
51 2016; Zimmerman et al., 2016; Jackson et al., 2017; Flannery et al., 2018). Each season, individuals in a defined community
52 cohort were recruited and tested for influenza when seeking outpatient care for acute respiratory infection. Eligibility was
53 restricted to individuals >6 months of age living near Marshfield who received routine care from the Marshfield Clinic. After
54 obtaining informed consent, a mid-turbinate swab was obtained for influenza detection. RT-PCR was performed using CDC
55 primers and probes to identify influenza cases, including type and subtype.

56 We sought to explain the variation in the age distribution of these cases by subtype and over time. Our model predicted
57 the relative number of cases of influenza in each birth year each season as a function of the age structure of the population,
58 age-specific differences in the risk of medically attended influenza A infection, early influenza infection, and vaccination.
59 Despite the extensive antigenic evolution in both subtypes over the study period, we found strong evidence of protection from
60 the subtype to which a birth cohort was likely first infected (the imprinting subtype) and variation in VE by birth cohort.

61 Results

62 The age distribution of cases varies significantly between seasons and subtypes

63 We examined the age distribution of cases of the dominant (most common) subtype in each season between 2007-2008
64 and 2017-2018 among enrolled patients. We excluded the subdominant subtype in each season due to concerns that short-
65 term interference between the subtypes (Laurie et al., 2015; Goldstein et al., 2011) would disproportionately affect the age
66 distribution of the rarer subtype. Differences between all pairs of seasons were evaluated by the G-test of independence and
67 corrected for multiple tests (Materials and Methods: "Calculating differences in the age distribution between seasons").

68 The age distribution of cases varies significantly between subtypes. The relative burden of cases is consistently higher
69 in people over 65 years old during H3N2-dominated seasons compared to H1N1-dominated seasons (Figure 1), and nearly
70 all H1N1-dominated seasons have significantly different age distributions from all H3N2-dominated seasons (Figure 1-
71 Supplement 1, off-diagonal quadrants).

72 The age distribution also varies significantly within subtypes over time (Figure 1-Supplement 1, diagonal quadrants).
73 The seven H3N2-dominated seasons display three types of age distributions (Figure 1-Supplement 1, white patches in upper
74 left-hand quadrant), and two correspond to major antigenic clusters (2007-2008 Fonville et al., 2015, 2010-2012 Ann et al.,
75 2012). These differences sometimes coincide with significant shifts in the age distribution between seasons. For instance, the
76 highest fraction of H3N2 cases occurs in 20-29 year olds in the 2007-2008 season, but this age group has the lowest fraction
77 of cases in the next H3N2-dominated season (2010-2011, Figure 1C). In H1N1, the shift from seasonal to pandemic strains is
78 associated with a significant change in the age distribution (Figure 1-Supplement 1, lower right-hand quadrant). The high
79 fraction of cases among 40-64 year-olds in the 2013-2014 season (Figure 1B) has been attributed to the emergence of strains
80 to which this group was especially susceptible (Linderman et al., 2014; Petrie et al., 2016).

81 We found further evidence that age groups differed in their susceptibility across seasons by examining the relative risk of
82 infection during the first versus second half of each epidemic period (Materials and Methods: "Calculating relative risk").
83 Because more susceptible populations experience higher attack rates, individuals in these populations should be infected
84 disproportionately early rather than late in an epidemic (Worby et al., 2015). We confirmed that an age group's relative risk of
85 infection in the first versus the second half of each epidemic correlates with the total fraction of cases in that age group that
86 season (Spearman's $\rho=0.41$, $p=0.001$, Figure 1-Supplement 2A). This trend is significant for H1N1 (Spearman's $\rho=0.47$,
87 $p=0.02$, Figure 1-Supplement 2A) and H3N2 seasons separately (Spearman's $\rho=0.35$, $p=0.05$, Figure 1-Supplement 2A). The
88 positive correlation in all seasons is robust to undersampling of cases at the start or end of specific seasons (Materials and
89 Methods: "Sensitivity to sampling effort", Figure 1-Supplement 2B). This provides supporting evidence that the different
90 numbers of cases in each age group reflect underlying differences in susceptibility.

91 Just as the age distribution of cases varies over time, the age groups with the highest relative risk of infection, and by
92 implication susceptibility, also change across seasons. For instance, 5-17 year olds had the highest relative risk of early

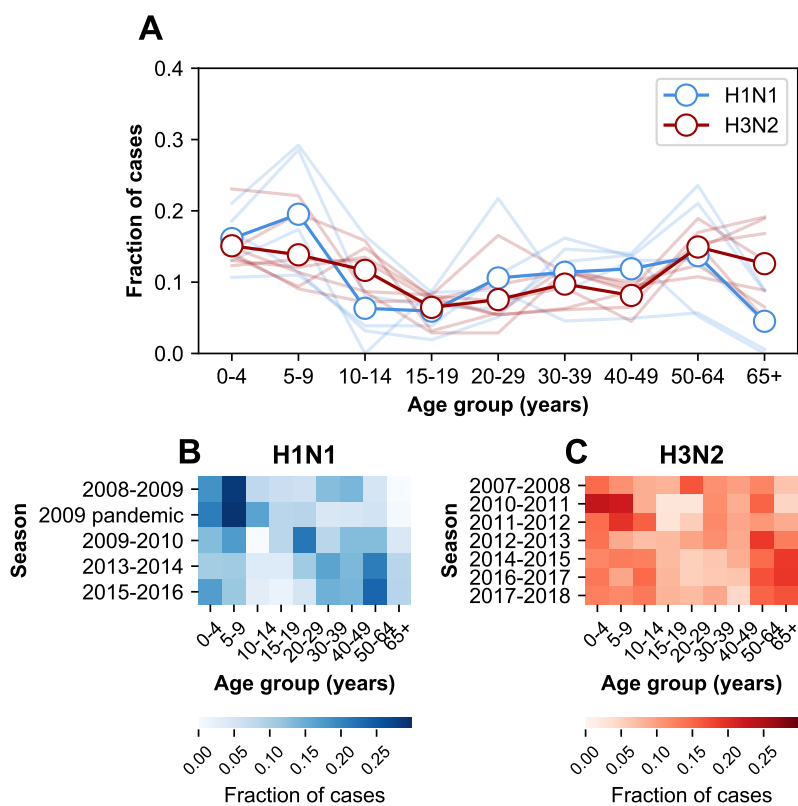


Figure 1. **A.** The age distributions of cases from the 2007-2008 through the 2017-2018 influenza seasons in Marshfield. Dark lines with open circles indicate the average fraction of cases in each age group. Lighter-colored lines show the age distribution for individual seasons. **B.** The age distribution of cases in H1N1-dominated seasons. **C.** The age distribution of cases in H3N2-dominated seasons.

93 infection in the 2008-2009 season, whereas 50-64 year-olds had the highest relative risk in the 2013-2014 season (Figure 1-
 94 Supplement 3). Relative risk in Marshfield is considerably more variable than national estimates, which showed that 5-17
 95 year-olds had the highest relative risk in all but one season from the 2009 pandemic to 2013-2014 (Worby et al., 2015). These
 96 differences may be due in part to the fact that our measurements of relative risk used outpatient visits, whereas the national
 97 estimates used hospitalizations.

98 Taken together, these findings suggest that the risk of influenza infection is not a simple function of age alone. Other
 99 factors, such as past influenza infections and vaccination, might explain the changing age distributions of cases in time.

100 **Imprinting probabilities of age groups change over time**

101 We hypothesized that variation in the age distribution of cases could be explained by the aging of birth cohorts with similar
 102 early exposure histories. This would cause the early exposure history of an age group to change in time. To calculate the
 103 probability that an individual in a particular age group had their first influenza A infection with a particular subtype, we
 104 adapted the approach from Gostic et al., 2016. Briefly, we calculated the probability that an individual born in a specific year
 105 had their first infection with H1N1, H2N2, or H3N2 using data on relative epidemic sizes and the frequencies of circulating
 106 subtypes (Figure 2-Supplement 1).

107 As expected, age groups' early exposures are not static and change over time (Figure 2). Older people nonetheless tend to
 108 be imprinted to H1N1 or H2N2, whereas younger people have higher probabilities of imprinting to H3N2. The effects of the
 109 2009 H1N1 pandemic are evident in the three youngest age groups as a transient increase (from 2009 to approximately 2013)
 110 in their H1N1 imprinting probability.

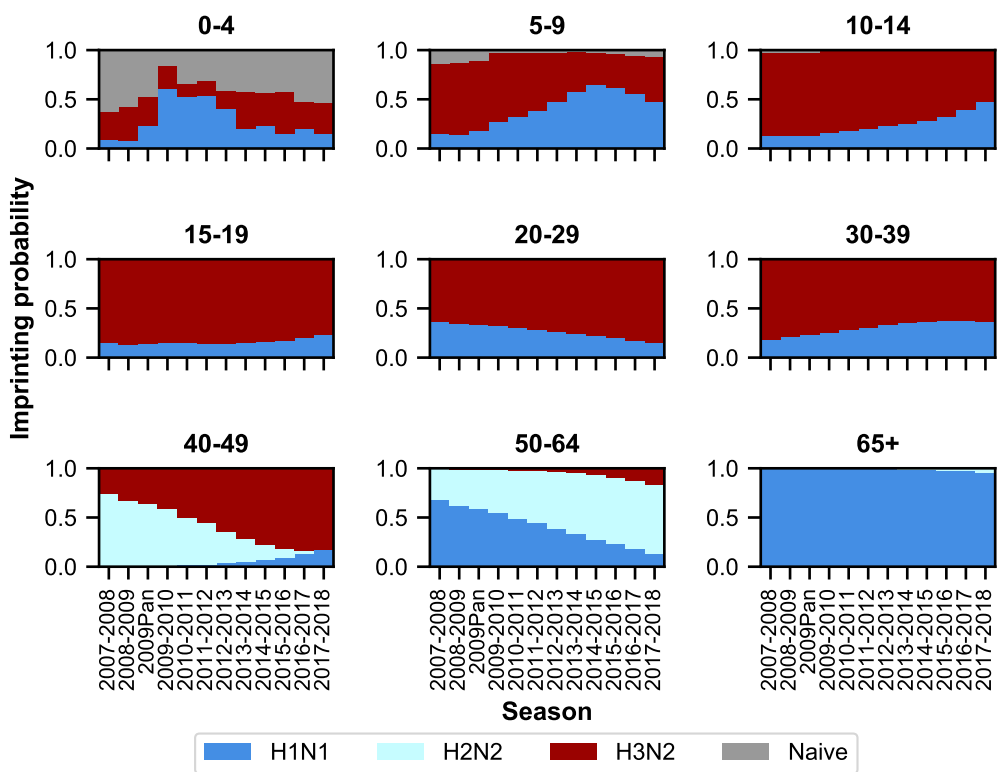


Figure 2. The imprinting probabilities of age groups change over time. Each panel shows the imprinting probabilities of an age group from the 2007-2008 season through the 2017-2018 season. The color of each bar corresponds to the imprinting subtype or naive individuals, who have not yet been infected.

111 **Modeling approach**

112 We fitted a set of models to estimate the effects of demography, age, imprinting, and vaccination on the age distribution
113 of influenza cases. The number of observed cases in influenza season t among people born in year y is proportional to a
114 combination of these factors:

- 115 1. *Demography*. The age distribution of our study cohort is not static over the study period. All models adjust for the
116 changing fractions of the population in each birth cohort and season (Figure 3-Supplement 1, Materials and Methods:
117 "Demography").
- 118 2. *Age-specific effects*. We consider that age itself may be associated with differences in influenza A infection risk
119 stemming from differences in susceptibility and/or rates of contact with infectious people. Additionally, we expect that
120 age groups may intrinsically differ in their healthcare-seeking behaviors. These factors are inseparable in our data, and
121 all models represent their combined effects with a static age-specific parameter shared by both subtypes that describes
122 the risk of age-specific medically attended influenza A infection (Materials and Methods: "Age-specific factors"). Thus,
123 we assume no intrinsic differences in the age-specific virulence of the two subtypes. These age-specific parameters
124 are fitted. We also adjust for other potential sources of age-specific bias, including age-specific differences in study
125 approachment and enrollment rates (Materials and Methods: "Age-specific factors").
- 126 3. *Imprinting*. We tested several hypotheses of how primary exposures could affect the risk of infection with H1N1 and
127 H3N2. In each version, we estimated fractional reductions in risk to H1N1 and H3N2 due to primary (i.e., imprinting)
128 exposure to the same type:
 - 129 • Subtype-specific imprinting: Influenza has two main antigens, hemagglutinin (HA) and neuraminidase (NA).
130 Imprinting could in theory derive from responses to either or both antigens. Because H1N1 is the only seasonal
131 subtype of influenza with N1, we cannot separate the effects of initial N1 exposure from initial H1 exposure.
132 However, since N2 appears in both H3N2 and H2N2 viruses, we can estimate protection against H3N2 infection
133 from initial N2 exposure separately from protection from initial H3 exposure (Materials and Methods: "HA
134 subtype imprinting" and "N2 imprinting").
 - 135 • Group-level imprinting: Influenza A viruses fall into two groups (I and II) corresponding to the two phylogenetic
136 clades of HA. Gostic et al., 2016 found that primary infection by a virus belonging to one group protected against
137 severe infection by another subtype in the same group. If group-level imprinting were influential, we would
138 see primary infection with H2N2 conferring protection against H1N1, another group I virus, as well as H1N1
139 protecting against H1N1 and H3N2 against H3N2. We considered a separate class of models that assumes
140 group-level protection instead of subtype-specific protection (Materials and Methods: "HA group imprinting").
- 141 4. *Vaccination*. Approximately 45% of the population of Marshfield is vaccinated against influenza each year. We
142 estimated cases in vaccinated and unvaccinated individuals of each birth year separately. Naively, we expect that
143 vaccinated individuals should seek medical attention for acute respiratory infection (ARI) proportionally to the fraction
144 of their cohort vaccinated that season. However, vaccinated individuals may seek medical attention for ARI more
145 frequently than expected due to positive associations between the decision to vaccinate, healthcare-seeking behavior,
146 and underlying medical conditions (Jackson et al., 2005a,b; Belongia et al., 2009). We attempted to adjust for this by
147 calculating the fraction of vaccinated people among those who had a medically attended acute respiratory infection
148 (MAARI) and tested negative for influenza (i.e., the test-negative controls, Materials and Methods: "Vaccination"). We
149 find that this correlates with but exceeds vaccination coverage for most age groups, suggesting vaccinated individuals
150 are overrepresented among cases for reasons unrelated to influenza (Figure 3-Supplement 2). We also assume that
151 vaccination is not perfectly effective, defining VE as the fractional reduction in cases expected in vaccinated compared
152 to unvaccinated individuals after controlling for the effects described above. We estimated subtype-specific VE under
153 five scenarios: (i) constant across age groups and seasons; (ii) season-specific and constant across age groups; (iii)
154 age-specific and constant across seasons; (iv) imprinting-specific; and (v) birth-cohort-specific. We assumed that
155 vaccination affects risk only in the current season, i.e., there are no residual effects from prior vaccination (Materials
156 and Methods: "Vaccination").

157 With these considerations, we evaluated the models by maximum likelihood and compared their performance using the
158 corrected Akaike information criterion (cAIC, Figure 3).

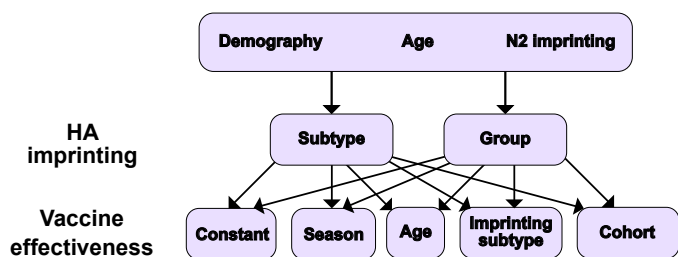


Figure 3. All models include demography, age effects, and the option of N2 imprinting. Ten different models result from considering different combinations of HA imprinting and VE.

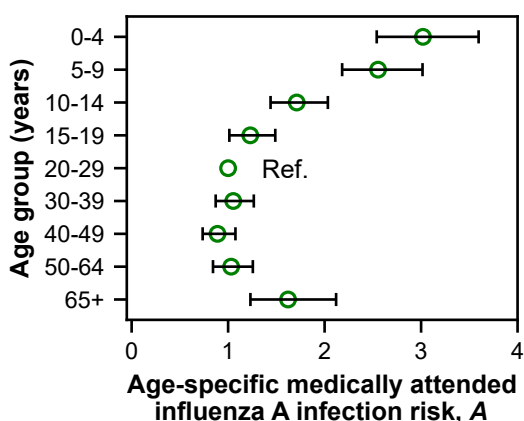


Figure 4. Open circles represent the maximum likelihood estimates of parameters describing age-specific differences in medically attended influenza A infection risk. Lines show the 95% confidence interval.

169 Age-specific differences in medically attended influenza A infection risk affect epidemic patterns

160 As expected, the cases reveal age-specific differences in the risk of medically attended influenza A infection. (Figure 4;
 161 Figure 4-Supplement 1; Appendix 1 Table 1). The risk of medically attended influenza A infection is roughly threefold higher
 162 among children less than four years old compared to adults 20-29 years old, after adjusting for other effects (Figure 4). This
 163 decline in risk with age is consistent with findings that attack rates decrease with age (Monto et al., 1985; Bodewes et al.,
 164 2011; Wu et al., 2010, 2017; Huang et al., 2019). Additionally, rates of healthcare-seeking behavior have been shown to
 165 decline with age before rising in adults over 65 years old (Biggerstaff et al., 2014; Brooks-Pollock et al., 2011; Van Cauteren
 166 et al., 2012), consistent with our results. Finally, the increased risk of medically attended influenza A infection among people
 167 ≥ 65 years old relative to other adults may be related to the increasing prevalence of high-risk medical conditions with age
 168 (Figure 4-Supplement 2).

169 Initial infection confers long-lasting, subtype-specific protection against future infection

170 Our best-fitting model supports subtype-specific imprinting for H1N1 and H3N2 (Figure 5, top row; Appendix 1 Table 1).
 171 The risk of future medically attended infection by H1N1 is reduced by 66% (95% CI 53-77%) in people imprinted to H1N1,
 172 whereas the risk of future medically attended infection by H3N2 is reduced by 33% (95% CI 17-46%) in people imprinted to
 173 H3N2. We found no evidence of a protective effect from imprinting to N2 (0%, 95% CI 0-7%). Our estimates of imprinting
 174 protection are insensitive to our choice of age groups for medically attended influenza A infection risk and VE (Appendix
 175 1 Table 3) as well as undersampling of influenza cases in some seasons (Figure 5-Supplement 1, Figure 5-Supplement 2,
 176 Materials and Methods, "Sensitivity to sampling effort").

177 We also tested whether vaccination is a plausible mechanism of imprinting (Figure 5-Supplement 3, Materials and
 178 Methods, "Calculating imprinting probabilities") and found that primary exposure via vaccination provided similar protection
 179 as imprinting from primary infection (100% of the effect of primary infection, 95% CI 74-100%, Figure 5-Supplement 4,

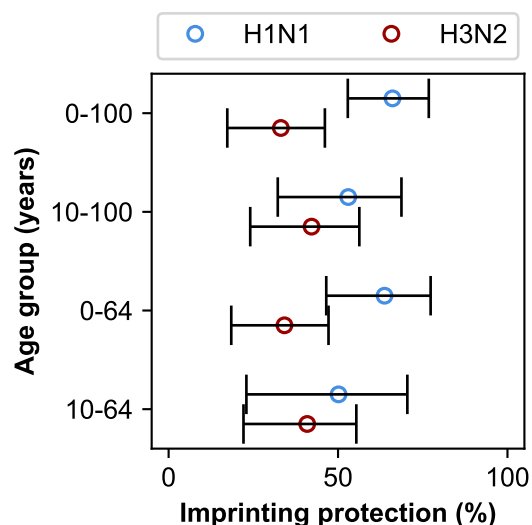


Figure 5. Imprinting is more protective against H1N1 infection than H3N2 infection. Open circles represent the maximum likelihood estimates of imprinting parameters from the best-fitting model for the indicated age group. Black lines show 95% confidence intervals.

180 Materials and Methods, "Vaccine imprinting"). However, the estimated protection could be confounded with residual
181 protection from prior season vaccination (Ohmit et al., 2014; McLean et al., 2014a,b) which the model excludes.

182 In theory, the protective effects of imprinting that we measured could be influenced by cross-protection rather than the
183 impact of first infection per se. Because first infections are also recent infections in children, we reasoned that the observed
184 imprinting effects might arise from confounding with recent infections in these ages. When we excluded the youngest age
185 groups, our estimates of H1N1 imprinting protection decreased while H3N2 imprinting protection increased (Figure 5, second
186 row). However, initial infection by H1N1 was still more protective than initial infection by H3N2, both imprinting effects
187 remained significantly positive, and there was no significant change in the values of other estimated parameters (Appendix 1
188 Table 1 and Table 2).

189 We expect that confounding with recent infection should also manifest in the difference between the observed and estimated
190 number of cases (i.e., the excess cases, Materials and Methods: "Calculating excess cases"), since our model does not take
191 prior season infections into account when estimating cases for the current season. More infections within a population in one
192 season should reduce susceptibility in that population at the start of the next season. We thus expect that a large number of
193 excess cases in one season will be followed by a small number of excess cases in the next season with the same dominant
194 subtype (i.e., a negative correlation). Instead, we observed that excess cases for each birth cohort have a weak positive
195 correlation from season to season, suggesting that immunity from recent infections is not a primary driver of variation in the
196 age distribution of cases (Figure 5-Supplement 5).

197 Since older adults have the highest probability of primary infection with H1N1, we also reasoned that older adults might
198 disproportionately drive the strong protection from H1N1 imprinting we observe. People born before 1947 were likely
199 exposed to H1N1 strains that are antigenically similar to the post-pandemic H1N1 strains that comprise most of our H1N1
200 infection data (Manicassamy et al., 2010; O'Donnell et al., 2012), creating the possibility that strain-specific cross-immunity
201 drives the pattern we attribute to subtype-specific imprinting. Excluding the oldest adults, however, does not significantly
202 change our estimates of imprinting protection or other parameters (Figure 5, third row, Appendix 1 Table 1, Table 2). When
203 we exclude both the youngest and oldest age groups, initial infections by H1N1 and H3N2 have similar protective effects
204 (Figure 5, bottom row). This shows that the combined effects of cross-protection in both the youngest and oldest individuals
205 contribute to the signal of imprinting protection we observe, but they are not its sole drivers.

206 **VE varies by birth cohort in older children and adults**

207 The best-fitting model includes age-specific VE (Figure 4-Supplement 1, Appendix 1 Table 2). While serological responses
208 to influenza vaccination are weakest in the young (Englund et al., 2005; Neuzil et al., 2006) and old (Lee et al., 2018;
209 DiazGranados et al., 2014), it is unclear what age-related factors would drive variation in VE in other age groups. We

210 hypothesized that VE in these ages is specific to exposure history, which correlates with birth year, rather than age.

211 To test this hypothesis, we fitted a model with birth-cohort-specific VE to data excluding either children <10 years old
212 or adults ≥ 65 years old. We chose birth cohorts that corresponded to the age groups of the original model in 2017-2018
213 (Materials and Methods: "Vaccination"), keeping the number of parameters the same (e.g., VE in the 20-29 age group became
214 VE in the 1988-1997 birth year cohort). We find that age-specific VE still outperforms all other models after we exclude the
215 oldest age group (≥ 65 years old). In contrast, birth-cohort-specific VE performs better when we exclude children <10 years
216 old (Figure 6-Supplement 1). Estimates of imprinting protection and age-specific risk of medically attended influenza in the
217 birth-cohort-specific VE models are not significantly different from estimates from the best-fitting model fitted to all ages
218 (Appendix 1 Table 1). Taken together, these results suggest that birth-cohort-specific VE best explains the case distribution in
219 older children and adults, who have likely experienced their first influenza infection, whereas age-specific VE best explains
220 cases in younger children, who have less influenza exposure.

221 VE differs between birth cohorts that have similar imprinting by subtype (Figure 6, Appendix 1 Table 4), suggesting that
222 specific infection history (beyond imprinting subtype) is important. For example, the 1968-1977 and 1988-1997 cohorts
223 have similar probabilities of primary exposure to H1N1 and H3N2, but they differ substantially in their VE to both subtypes
224 (Figure 6). The 1988-1997 and 1998-2002 cohorts also have similar probabilities of primary exposure to each subtype and
225 have similar H1N1 VEs, but have significantly different H3N2 VEs (Figure 6). Antigenic differences within each subtype
226 might explain this variation.

227 Our results support the idea that biases in immune memory from early exposures (i.e., original antigenic sin; Davenport
228 and Hennessy, 1957; Francis, 1960; Groth and Webster, 1966) influence VE. The model with birth-cohort-specific VE better
229 estimates cases among vaccinated 50-64 year-olds (born 1953-1967) in the 2015-2016 season than the model with age-specific
230 VE (Figure 6-Supplement 2, Materials and Methods: "Calculating excess cases"). Reduced VE in this age group has been
231 attributed to the exacerbation of antigenic mismatch by the vaccine in adults whose antibody responses were focused on a
232 non-protective site (Skowronski et al., 2017b; Flannery et al., 2018). The improved performance of birth-cohort-specific VE
233 relative to age-specific VE suggests other seasons and age groups where original antigenic sin might have influenced VE,
234 such as 20-29 year-olds in the 2007-2008 influenza season.

235 **Discrepancies partly explained by antigenic evolution**

236 The best-fitting model accurately reproduces the age distributions of vaccinated and unvaccinated cases of each subtype,
237 aggregated across seasons (Figure 7A). The only exception is that it underestimates H1N1 cases in unvaccinated 5-9 year-olds.
238 By examining the differences between predicted and observed cases for each season, we see that this is largely driven by
239 infection during the 2009 H1N1 pandemic (Figure 7B). Such a large antigenic change may have negated any protection from
240 previous infection in 5-9 year-olds and made them particularly susceptible to pandemic infection.

241 The model underestimates cases in unvaccinated individuals >30 years old in the 2013-2014 season. This is further
242 evidence that subtype-specific imprinting cannot explain all age variation. As mentioned before, this season provided one of
243 the first examples that original antigenic sin could affect protection: middle-aged adults had been targeting a familiar site
244 on the pandemic strain that then mutated; other age groups were effectively blind to these changes, owing to their different
245 exposure histories (Linderman et al., 2014; Huang et al., 2015; Arriola et al., 2014; Dávila et al., 2014; Petrie et al., 2016).

246 **Discussion**

247 The distribution of influenza cases by birth year is consistent with subtype-level imprinting, whereby initial infection with a
248 subtype protects against future infections by the same subtype. The stronger protective effect observed for primary H1N1
249 infection compared to primary H3N2 infection may be caused by greater cross-protective responses to conserved epitopes.
250 This is in line with previous work modeling antibody titer dynamics that showed that protection conferred by H1N1 infection
251 is longer-lasting than protection conferred by H3N2 infection (Ranjeva et al., 2019). Subtype-specific protection is more
252 specific than the previously reported group-level imprinting (Gostic et al., 2016) but clearly arises from primary infection
253 rather than any prior exposure.

254 In contrast to the clear role of the imprinting subtype in protection from infection, the model implicates the imprinting
255 strain or other attributes of exposure history in VE. Birth-cohort-specific VE predicts the distribution of cases in older children
256 and adults better than age-specific or imprinting-subtype-specific VE. Although seasonal estimates of VE routinely stratify
257 by age, shifts in VE from one season to the next might be easier to interpret in light of infection history (e.g., Skowronski
258 et al., 2017b; Flannery et al., 2018). The results suggest this effect may be complex, i.e., influenced by strains' specific

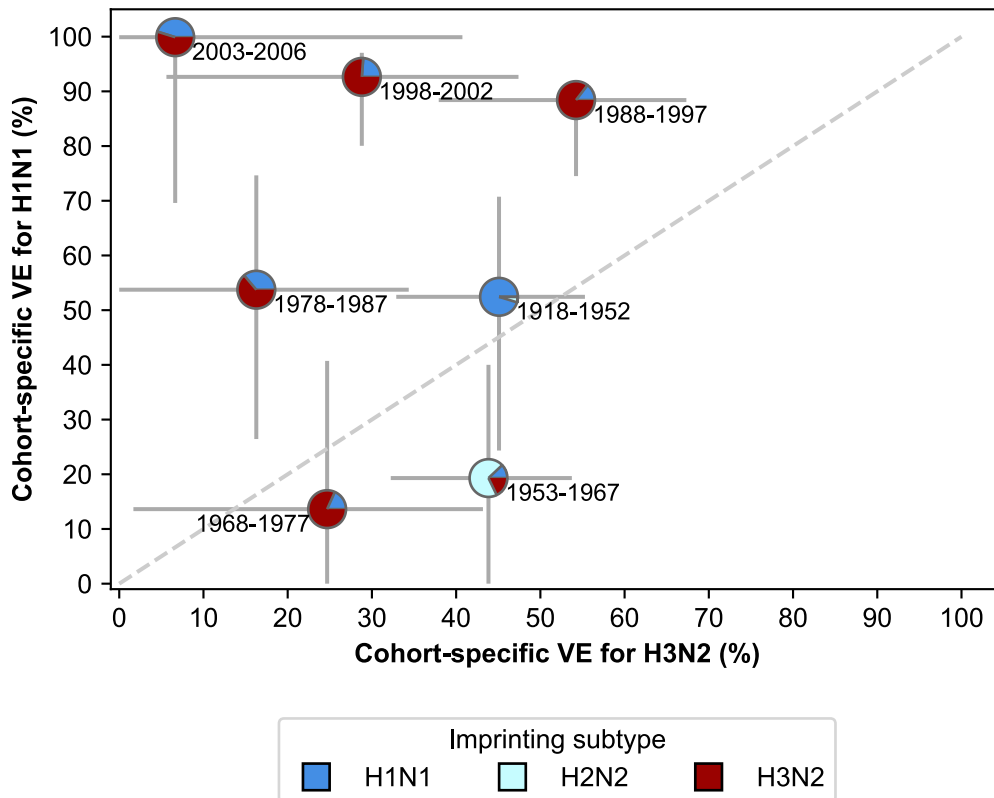


Figure 6. Birth-cohort-specific VE differs significantly between subtypes and birth cohorts. The location of each pie chart represents the H3N2 (x-axis) and H1N1 (y-axis) VE estimates for a birth cohort (indicated by text) obtained from our model excluding children <10 years old. Pie charts are colored by the probability of first infection by each subtype (i.e., imprinting probability). 95% confidence intervals of the VE estimates are indicated by light grey solid lines. The dashed grey line shows the diagonal where the VE estimate for H1N1 is equal to the VE estimate for H3N2.

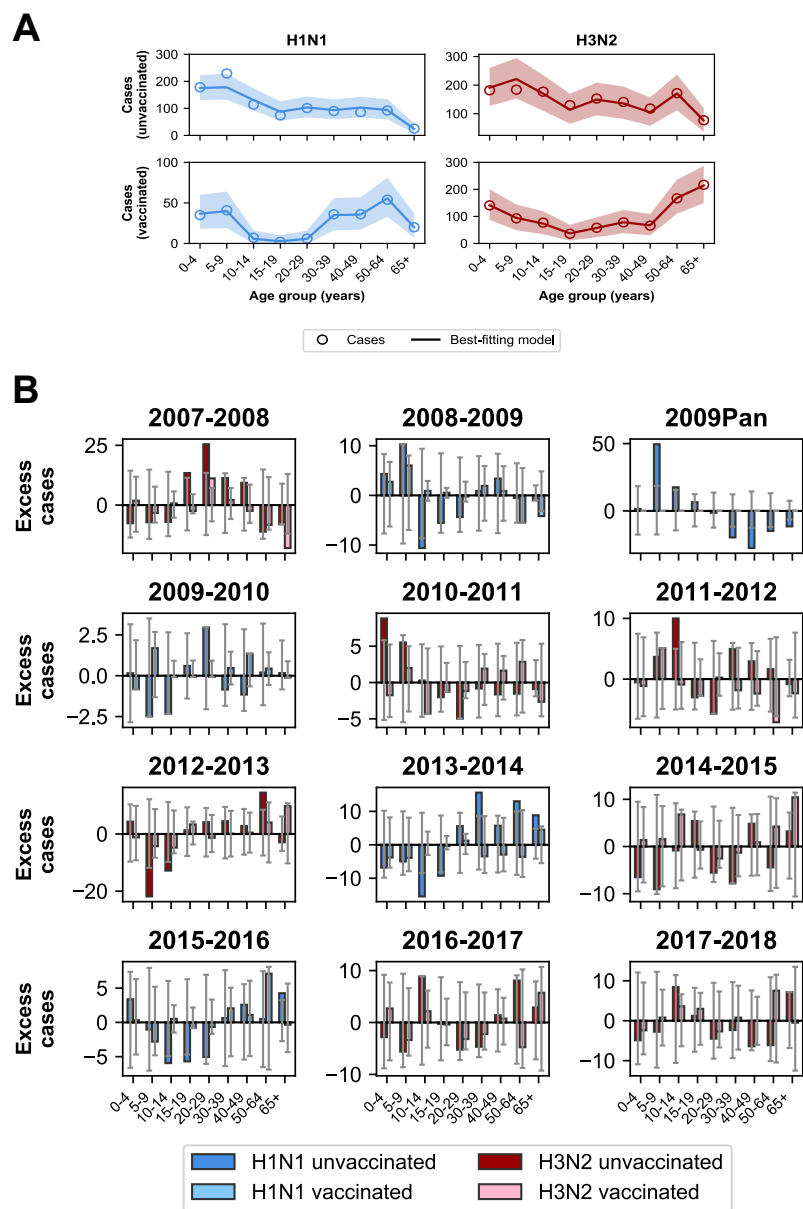


Figure 7. A. Best-fitting model accurately predicts the overall age distribution of cases across seasons and age groups. The best-fitting model includes the effects of demography, age, VE by age class, and subtype-specific HA imprinting. Each row depicts the age distribution of cases among unvaccinated (top) and vaccinated (bottom) individuals over all sampled seasons (2007-2008 through 2017-2018). Each column indicates H1N1 cases (left, blue) and H3N2 cases (right, red). Open circles represent observed cases, solid lines represent the predicted number of cases from the best-fitting model, the shaded area represents the 95% prediction interval of the best-fitting model. **B.** Excess cases of dominant subtype for each season. Each panel shows the excess cases of the dominant subtype for each age group among unvaccinated (dark bars) and vaccinated (light bars) individuals. Excess cases are defined as the predicted number of cases from the best-fitting model - observed cases. Grey error bars show the 95% prediction interval.

259 identities rather than merely their subtype. Our model cannot distinguish between the possibility that the precise identity of
260 the imprinting strain primarily determines later VE, or if individuals' responses to vaccination are shaped by a particular
261 succession of exposures, which will be common to others in the same birth cohort. Regardless, variation in VE between birth
262 cohorts appears substantial and suggests a role for past exposure in the effectiveness of vaccination. This presents a challenge
263 for the improvement of vaccination strategies (Erbelding et al., 2018).

264 Biases associated with our methodology and the vaccination history of our study population may confound our estimates
265 of VE. Potential selection and misclassification biases are associated with studies that use influenza test-negative controls
266 to control for differences in healthcare-seeking behavior (Lewnard et al., 2018; Sullivan et al., 2016). Because we also use
267 test-negative controls to set our null expectation for the distribution of cases among birth cohorts, our VE estimates are subject
268 to these biases as well. Moreover, our study population is heavily vaccinated, and the most participants are frequent vaccinees
269 (Figure 3-Supplement 3). Frequent vaccination has been associated with reduced VE (McLean et al., 2014b; Saito et al.,
270 2018; Skowronski et al., 2016). Therefore, the model may underestimate VE in less vaccinated populations. We observed an
271 unusually high H1N1 VE in the 2003-2006 birth cohort. Because we restricted cases in this analysis to people ≥ 10 years old,
272 this VE estimate included data from only the 2013-2014 and 2015-2016 influenza seasons. No H1N1 cases among vaccinated
273 or unvaccinated individuals were observed in this birth cohort for those seasons, which in turn led to this high estimate of
274 H1N1 VE. To reduce stochastic effects, our estimates are worth repeating in a larger population.

275 Incorporating differences in susceptibility based on exposure history might improve methods to forecast influenza seasons.
276 Our analysis of the relative risk of infection during the first half of each season shows more variation in the most susceptible
277 age groups from season to season than previously estimated (Worby et al., 2015). While the smaller sample sizes in Marshfield
278 compared to national data create uncertainty in our estimates, the correlation between the relative risk and total fraction of
279 cases indicates that the age groups driving epidemics change from season to season. As our results show, these differences in
280 susceptibility may derive from differences in exposure history. Therefore, incorporating information on exposure history into
281 epidemic models may allow for more accurate identification of at-risk populations.

282 While the rate of antigenic evolution affects the rate at which different populations become susceptible to infection, the
283 heterogeneity in susceptibility we observe here may also drive antigenic evolution. This heterogeneity in susceptibility implies
284 that influenza viruses face different selective pressures in groups with different exposure histories (Cobey and Hensley, 2017).
285 Recent research consistent with this hypothesis has shown that sera isolated from different individuals can select for distinct
286 influenza escape mutants (Lee et al., 2019). More careful study of how immune memory to influenza evolves from infection
287 and vaccination might improve understanding of influenza's evolution.

288 **Materials and Methods**

289 **Study cohort**

290 Cases of PCR-confirmed, medically attended influenza were identified from annual community cohorts based on residency in
291 the Marshfield Epidemiologic Study Area (MESA) in central Wisconsin. MESA is a 14-ZIP-code geographic area surrounding
292 Marshfield, Wisconsin, where nearly all residents receive outpatient and inpatient care from the Marshfield Clinic Health
293 System. For each influenza season from 2007-2008 through 2017-2018, we identified a subset of MESA residents >6 months
294 of age who received routine care from the Marshfield Clinic. These individuals were eligible for recruitment into a VE study
295 if they sought care for acute respiratory illness during each influenza season. Most patients with MAARI were recruited in
296 the outpatient setting, but inpatient recruitment also occurred in 2007-08 and 2008-09. Recruitment occurred in primary
297 care departments, including urgent care, pediatrics, combined internal medicine and pediatrics, internal medicine, and family
298 practice. The proportion of patients with MAARI who were screened for enrollment varied by season. We excluded patients
299 recruited in an inpatient (hospital) setting.

300 Each season, recruitment began when influenza activity was detected in the community and usually continued for 12-15
301 weeks. Symptom eligibility criteria varied by season but included fever/feverishness or cough during most seasons. We
302 retroactively standardized symptom eligibility criteria to only require cough as a symptom. Individuals with illness duration
303 >7 days were excluded. After obtaining informed consent, a mid-turbinate swab was obtained for influenza detection. RT-PCR
304 was performed using CDC primers and probes to identify influenza cases, including type and subtype.

305 The Marshfield Clinic generally does not capture MAARI in nursing facilities with dedicated medical staff, causing
306 undersampling of the oldest age groups. We adjusted for this ("Age-specific factors" below).

307 We considered subjects vaccinated if they received that season's influenza vaccine ≥ 14 days before enrollment. For the

308 2009-2010 season, we only considered receipt of the 2009 monovalent vaccine.

309 **Calculating differences in the age distribution between seasons**

310 We defined the age distribution of each season as the number of cases of the dominant subtype in each of nine age groups (0-4
311 year-olds, 5-9 year-olds, 10-14 year-olds, 15-19 year-olds, 20-29 year-olds, 30-39 year-olds, 40-49 year-olds, 50-64 year-olds,
312 and >64 years old). The G-test of independence was used to determine whether each pair of seasons had significantly different
313 age distributions. We considered differences significant if the Bonferroni-corrected p-value was <0.05.

314 **Calculating relative risk**

315 We used an approach similar to Worby et al., 2015 in calculating relative risk. We defined the midpoint of each season as the
316 week in which the cumulative number of cases of the dominant subtype exceeded 50% of the total for that season. Weeks
317 before and after this point were assigned to the first and second half of the season, respectively. We assigned each case to one
318 of the five age groups used by Worby et al., 2015 (0-4 year-olds, 5-17 year-olds, 18-49 year-olds, 50-64 year olds, and >64
319 years old). For each age group g , we defined relative risk as

$$\frac{C_{\text{first},t,g}}{C_{\text{second},t,g}},$$

320 where $C_{\text{first},t,g}$ and $C_{\text{second},t,g}$ are the fraction of cases of the dominant subtype in age group g during influenza season t that
321 occurred during the first or second half of the season, respectively. A relative risk >1 indicates that cases in an age group
322 were more likely to occur during the first half of the season.

323 **Calculating imprinting probabilities**

324 **Seasonal intensity**

325 We define the intensity of an influenza season as the product of the mean fraction of patients with influenza-like illness (ILI)
326 and the percentage of specimens testing positive for influenza A that season,

$$I_t = \frac{ILI_t F_t}{N_t},$$

327 where ILI_t is the mean fraction of all patients with ILI in season t adjusted for differences in state population size (CDC,
328 2018), F_t is the number of respiratory specimens testing positive for influenza A in season t , and N_t is the total number of
329 respiratory specimens tested in season t . For seasons 1997-1998 through 2017-2018, these data were obtained from the U.S.
330 Outpatient Influenza-like Illness Surveillance Network (ILINet) and the World Health Organization/National Respiratory
331 and Enteric Virus Surveillance System (WHO/NREVSS) Collaborating Labs (CDC, 2018). For seasons 1976-1977 through
332 1996-1997, we assumed that the mean ILI was equal to the mean of mean ILI for seasons 1997-1998 through 2017-2018. We
333 obtained data on F_t and N_t for these seasons from Thompson et al., 2003. We then normalized the intensity of each season by
334 dividing I_t by the mean of I_t from the 1976-1977 through 2017-2018 seasons. For all seasons before 1976-1977, we assumed
335 that the intensity of influenza A equalled the mean intensity of seasons 1976-1977 through 2017-2018.

336 **Fraction of season experienced**

337 We define the fraction of a given influenza season $f_{w,t}$ occurring in week w of season t as

$$f_{w,t} = \frac{ILI_{w,t} F_{w,t}}{N_{w,t} \sum_{w'=w_0}^{w_f} \frac{ILI_{w',t} F_{w',t}}{N_{w',t}}},$$

where $ILI_{w,t}$ is the weighted fraction of all patients with ILI in week w of season t , $F_{w,t}$ is the number of respiratory specimens
testing positive for influenza A in week w of season t , and $N_{w,t}$ is the number of specimens tested in week w of season
 t . $\sum_{w'=w_0}^{w_f} \frac{ILI_{w',t} F_{w',t}}{N_{w',t}}$ is the product of ILI and the fraction of positive influenza A specimens summed over all weeks of the
influenza season t , where w_0 is the first week of the season and w_f is the final week of the season. We define the start of
the influenza season as week 40 of the calendar year, which usually falls at the beginning of October. For seasons before
1997-1998, where weekly data is unavailable, we assume that the fraction of the influenza season experienced in week w is

$$f_{w,t} = \bar{f}_{w,t},$$

338 where $\bar{f}_{w,t}$ is the mean fraction of the influenza season experienced at week w for all seasons after 1997-1998.

339 We use $f_{w,t}$ to calculate the fraction of an influenza season experienced by an individual born in year y . We assume that
 340 people born in year y are born randomly throughout the year. We also assume that due to maternal immunity, infants do not
 341 experience immunizing exposure to influenza until they are at least 180 days old. Let $p_{y,w,t}$ be the proportion of individuals
 342 born in year y that are over 180 days old in week w of season t and $e_{y,t}$ be the fraction of individuals born in year y exposed to
 343 influenza season t . Then

$$e_{y,t} = \sum_{w=w_0}^{w_f} f_{w,t} p_{y,w,t}.$$

344 Imprinting probability

345 We emulate the approach of Gostic et al., 2016 in calculating the probability that people born in a particular year had their
 346 initial influenza exposure to a particular subtype.

347 To obtain imprinting probabilities, we calculate the probability that an individual born in year y receives their first
 348 influenza A exposure in influenza season t . Specifically, we consider two possible scenarios. First, we assume that only
 349 infections result in an imprinting exposure. Second, we modify our calculation to include the possibility that both vaccination
 350 and infection result in an imprinting exposure.

351 We set the probability of infection for naive individuals at 0.28 (Bodewes et al., 2011; Gostic et al., 2016). Using this
 352 probability, we can calculate a per-season attack rate a assuming an exponential hazard:

$$a = -\ln(0.72).$$

353 We then scale this attack rate by the intensity of influenza season t (I_t) and the fraction of influenza season t experienced
 354 by an individual born in year y ($e_{y,t}$, "Seasonal intensity" above). The probability that a naive individual born in year y is
 355 infected in influenza season t is

$$p_{y,t} = 1 - e^{-I_t e_{y,t} a}.$$

356 Considering only infection,

$$Pr(\text{unexposed}, t) \equiv N(t)$$

$$N(t=0) = 1$$

$$Pr(\text{first exposure in season } t) = Pr(\text{infected}|\text{unexposed})Pr(\text{unexposed}) = p_{y,t}N(t)$$

$$N(t+1) = N(t)(1 - p_{y,t})$$

357 We calculate subtype-specific imprinting probabilities by multiplying $p_{y,t}N(t)$ by the subtype frequencies for each season
 358 (Figure 2-Supplement 1).

359 To incorporate vaccination, we make a simplifying assumption that for all seasons except the 2009 pandemic and the
 360 2009-2010 influenza seasons (discussed below), vaccination occurs before infection. We also consider that given vaccination
 361 coverage for a particular birth cohort and season ($c_{y,t}$), only a fraction of those individuals will be receiving their first
 362 vaccination because people who get vaccinated are more likely to get vaccinated again. We calculated this probability of first
 363 vaccination by age ($f_{a,t}$) using the vaccination status of children enrolled in our study (Figure 5-Supplement 7).

364 We track the fraction of a birth cohort naive to any exposure ($N(t)$ as above) and the fraction of a birth cohort naive to
 365 vaccination ($N_v(t)$). Therefore, to calculate imprinting probabilities, we first consider vaccination:

$$N(t=0) = N_v(t=0) = 1$$

$$Pr(\text{first vaccination in season } t) = \frac{Pr(\text{vaccinated})Pr(\text{first vaccination}|\text{vaccinated})}{Pr(\text{naive to vaccination})} = \frac{c_{y,t}f_{a,t}}{N_v(t)}$$

$$Pr(\text{first exposure via vaccination in season } t) = \frac{c_{y,t}f_{a,t}}{N_v(t)} N(t)$$

$$N_v(t+1) = N_v(t)\left(1 - \frac{c_{y,t}f_{a,t}}{N_v(t)}\right)$$

366 Then, we update $N(t)$ to reflect vaccination and use this new value of $N(t)$ to calculate the fraction of people infected:

$$N(t) = N(t) \left(1 - \frac{c_{y,t} f_{a,t}}{N_v(t)}\right)$$

$$Pr(\text{first exposure via infection in season } t) = Pr(\text{infected}|\text{unexposed})Pr(\text{unexposed}) = p_{y,t}N(t)$$

$$N(t+1) = N(t)(1 - p_{y,t})$$

367 During the 2009 H1N1 pandemic and 2009-2010 seasons, infection, vaccination with the seasonal vaccine, and vaccination
368 with the monovalent vaccine occurred simultaneously. Therefore, we used weekly rates of vaccination and infection to estimate
369 the probability that an individual's first exposure for that season was infection, seasonal vaccination, or monovalent vaccination.

370 Vaccination coverage

371 Seasonal influenza vaccination coverage for MESA Central was collected by age in the 2007-2008 through 2017-2018 seasons
372 using a real-time immunization registry (Irving et al., 2009). Monovalent vaccination coverage for the 2009-2010 season was
373 obtained by directly measuring monovalent vaccination coverage in enrolled individuals and fitting a smoothing spline to the
374 data (Figure 5-Supplement 6).

375 For seasons before 2007-2008, we used U.S. national data on vaccination coverage in children (2002-2003 through
376 2003-2004; Santibanez et al., 2006, 2004-2005 through 2006-2007; Santibanez et al., 2014). We assumed that vaccination
377 coverage in children (i.e., potentially imprinting vaccination) was 0 before the 2002-2003 season, since that was the first
378 season in which the Advisory Committee on Immunization Practices encouraged children 6-23 months old to receive influenza
379 vaccination (Bridges et al., 2002).

380 Model components

381 We aim to infer $p_{s,t,y,v}$, the predicted fraction of all PCR-confirmed influenza cases of dominant subtype s in influenza season t
382 among people born in year y with vaccine status v .

383 We normalize all models such that for each season t , $\sum_{y=1918}^{y_{\max}} p_{s,t,y,\text{unvac.}} + \sum_{y=1918}^{y_{\max}} p_{s,t,y,\text{vac.}} = 1$. Let $p'_{s,t,y,v}$ be the unnormal-
384 ized proportions. Then for season t ,

$$p_{s,t,y,v} = \frac{p'_{s,t,y,v}}{\sum_{y=1918}^{y_{\max}} p_{s,t,y,\text{unvac.}} + \sum_{y=1918}^{y_{\max}} p_{s,t,y,\text{vac.}}}$$

For convenience, let $k_{M,t}$, the normalizing constant for season t in model M , be

$$k_{M,t} = \frac{1}{\sum_{y=1918}^{y_{\max}} p_{s,t,y,\text{unvac.}} + \sum_{y=1918}^{y_{\max}} p_{s,t,y,\text{vac.}}}$$

385 Demography

386 We used Marshfield-specific data on the age distribution for each season (Kieke et al., 2015). Individuals ≥ 90 years old were
387 grouped into a single age class. We therefore estimated the number of people in each age by assuming a geometric decline in
388 the age distribution. We converted the raw age distribution for each season into a distribution by birth year by distributing
389 people of a specific age into the two possible birth years of that age in a specific season. Specifically, we assumed that people
390 were born uniformly throughout the year. We defined a breakpoint date prior to the start of the enrollment period based
391 on when the 6 month-old age limit cutoff was set (e.g., if the breakpoint date was October 1, then infants had to be 6
392 months old by that date to be eligible for enrollment). We used this date to calculate the fraction of people of age a in season t
393 who were born in year $t - y$ ($f_{1,a,t}$) or year $t - y - 1$ ($f_{2,a,t}$). A fraction $f_{1,a,t}$ of the total population of age a in season t
394 assigned to birth year $t - y$ and $f_{2,a,t}$ to $t - y - 1$. Breakpoint dates ranged from September 1 through January 1 with the
395 exception of the pandemic season which had a breakpoint date of May 1, 2009. The start of the enrollment period ranged
396 from December to January with the exception of the 2009 pandemic season, when enrollment began in May 2009. For the
397 2009 pandemic season, we assumed that the age distribution was the same as the 2008-2009 season. The above procedure
398 allows us to calculate $D_{t,y}$, the fraction of people born in year y during influenza season t . Therefore,

$$p_{s,t,y,v} \propto D_{t,y}$$

399 Age-specific factors

400 We modeled age-specific differences in influenza infection risk and healthcare-seeking behavior by using parameters that
401 represent the relative risk of medically attended influenza A infection in each age group. These parameters combine the effects
402 of underlying age-specific differences in influenza A infection risk as well as age-specific differences in healthcare-seeking
403 behavior. We consider the same age groups as before (0-4 year-olds, 5-9 year-olds, 10-14 year-olds, 15-19 year-olds, 20-29
404 year-olds, 30-39 year-olds, 40-49 year-olds, 50-64 year-olds, and >64 years old). We choose 20-29 year-olds as our reference
405 age group. All age groups aside from 20-29 year-olds have an associated parameter that models their risk of medically
406 attended influenza A infection relative to 20-29 year-olds. These parameters can take on any positive value. To map these
407 age-specific parameters to birth cohorts, we consider that each birth cohort has two possible ages in each season (a_1 and a_2).
408 Let $G(a)$ be a function that specifies the age group g of a given age a . Then $A_{t,y}$ the age-specific risk of medically attended
409 influenza A infection for a person born in year y in season t is

$$A_{t,y} = f_{a_1,t,y}A_{G(a_1)} + f_{a_2,t,y}A_{G(a_2)}$$

410 where $f_{a_1,t,y}$ and $f_{a_2,t,y}$ are the fractions of birth cohort y who are age a_1 or a_2 in influenza season t , and $A_{G(a_1)}$ and $A_{G(a_2)}$ are
411 the age-group-specific parameters for a_1 and a_2 . With this, we model age-specific effects as

$$p_{s,t,y,v} \propto A_{t,y}.$$

412 The relative rates at which different age groups were approached for study enrollment (the approachment rate, p_{approach})
413 varied between seasons. Similarly, the relative rates at which different age groups enrolled in the study after being approached
414 (the enrollment rate, p_{enroll}) also varied between seasons. Enrollment rates also varied between vaccinated and unvaccinated
415 individuals.

416 We defined the approachment rate of an age group g in season t as

$$p_{\text{approach},t,g} = \frac{N_{\text{approached},t,g}}{N_{\text{MAARI},t,g}},$$

417 where $N_{\text{approached},t,g}$ is the number of people in age group g during season t who were approached for enrollment, and $N_{\text{MAARI},t,g}$
418 is the total number of people in the Marshfield cohort who presented with MAARI regardless of whether they were approached
419 for enrollment.

420 We defined the enrollment rate of age group g in season t with vaccination status v as

$$p_{\text{enroll},t,g,v} = \frac{N_{\text{enrolled},t,g,v}}{N_{\text{approached},t,g,v}}$$

421 where $N_{\text{enrolled},t,g,v}$ is the number of people in age group g with vaccination status v who enrolled in the study in season t , and
422 $N_{\text{approached},t,g,v}$ is the number of people in age group g with vaccination status v who were approached for enrollment in season
423 t . Due to differences in data collection for the 2007-2008 and 2008-2009 seasons, complete vaccination records for eligible
424 unenrolled individuals were not available, so we assumed that the enrollment rates by age group and vaccination status in
425 those seasons were equal to the mean enrollment rate for each age group and vaccination status across all other seasons.

426 We normalized $p_{\text{approach},t,g}$ by the value of $p_{\text{approach},t,g}$ for the reference age group (i.e., 20-29 year-olds) in each season.
427 Similarly, we normalized $p_{\text{enroll},t,g,v}$ to the value of $p_{\text{enroll},t,g,v}$ for unvaccinated members of the reference age group for each
428 season. This yielded the relative approachment and enrollment rates $p'_{\text{approach},t,g}$ and $p'_{\text{enroll},t,g,v}$. We converted both $p'_{\text{approach},t,g}$
429 and $p'_{\text{enroll},t,g,v}$ to birth-year specific covariates (i.e. covariates by y instead of g) using the same procedure described above for
430 the estimated age-specific parameters.

431 Finally, the study did not enroll residents of skilled nursing facilities with dedicated medical staff. To account for this, we
432 estimated the proportion of the population in nursing facilities within the study area. We obtained the total number of beds in
433 nursing facilities within the Marshfield study area in 2018 from the Wisconsin Department of Health Services (WDHS, 2018).
434 We assumed that the total number of beds did not change between 2007-2008 and 2017-2018. We also used data from the
435 Centers for Medicare and Medicaid Services (CMS, 2015) to calculate the percent of beds occupied in Wisconsin nursing
436 facilities by age for 2011 through 2014 and the fraction of people in a nursing facility by age group. We used a smoothing
437 spline to obtain the fraction of people of a given age in a nursing facility. For seasons before 2010-2011 and after 2013-2014,
438 we assumed that the fraction of people of a given age in a nursing facility was the average value for 2011-2014. Given the

439 total population of the study area by age and season, we could then calculate the fraction of people in a given age a and season
 440 t who are in nursing facilities ($s_{t,a}$). We convert this to a covariate by birth year ($s_{t,y}$) using the same procedure described
 441 above for the age-specific parameters.

442 Thus, the combination of estimated age-specific effects and age-specific covariates is modeled as

$$p_{s,t,y,v} \propto A_{t,y} p'_{\text{approach},t,y} p'_{\text{enroll},t,y,v} (1 - s_{t,y}).$$

443 Vaccination

444 Vaccinated individuals may seek healthcare for symptomatic influenza at a different rate than unvaccinated individuals.
 445 Moreover, because vaccines are routinely recommended for individuals with underlying health conditions, pre-existing
 446 susceptibility to acute respiratory infection among vaccinated individuals may also differ from unvaccinated individuals. Let
 447 $R_{t,g}$ represent the fraction of vaccinated individuals in age group g in season t that present with MAARI. We use test-negative
 448 controls to estimate this as

$$R_{t,g} = \frac{v_{t,g}^-}{u_{t,g}^- + v_{t,g}^-},$$

449 where $v_{t,g}^-$ and $u_{t,g}^-$ are the number of vaccinated or unvaccinated individuals born in year g presenting with MAARI and
 450 testing negative for influenza in season t . We compared this quantity to the vaccination coverage of age group g in season t ,
 451 $c_{t,g}$ (Figure 3-Supplement 2).

452 We converted $R_{t,g}$ to $R_{t,y}$ (i.e., to a birth cohort-indexed covariate) using the same procedure described above to convert
 453 age group-specific parameters to birth-cohort-specific parameters.

454 We tested five different VE schemes: subtype-specific VE that remained constant across seasons and cohorts (2 parameters),
 455 subtype-specific VE that varied between the age groups described above (18 parameters), VE that varied between seasons (12
 456 parameters), VE for each possible imprinting subtype (6 parameters), and birth-cohort-specific VE (18 parameters). These
 457 VE parameters (V) reduce the probability of medically attended influenza A infection among vaccinated individuals within a
 458 birth cohort, i.e.,

$$p_{s,t,y,\text{vac}} \propto R_{t,y} V,$$

$$p_{s,t,y,\text{unvac}} \propto (1 - R_{t,y}),$$

459 where V depends on the specific implementation of VE used.

460 For constant VE, $V = V_s = 1 - v_s$.

461 For season-specific VE, $V = V_{s,t} = 1 - v_{s,t}$.

462 For age-specific VE, we use a similar approach as described above for the age-specific parameters. We use the same age
 463 classes but do not consider a reference age class, so that each age group has an associated VE parameter for each subtype.
 464 Therefore,

$$V = V_{s,t,y} = 1 - (f_{a1,t,y} v_{G(a1),s} + f_{a2,t,y} v_{G(a2),s}),$$

465 where $v_{G(a1),s}$ and $v_{G(a2),s}$ are age-specific VE parameters for $a1$ and $a2$. Recall that the function G specifies an age group for a
 466 given age.

467 For imprinting-specific VE, we use the imprinting probabilities for each birth cohort described above such that

$$V = V_{s,t,y} = \prod_{z \in \{\text{H1N1}, \text{H2N2}, \text{H3N2}\}} (1 - v_{s,z} m_{z,t,y}),$$

468 where $v_{s,z}$ is the VE among people imprinted to subtype z against infection by dominant subtype s , and m_z is the imprinting
 469 probability for subtype z in season t for birth cohort y .

470 For birth-cohort-specific VE, we defined nine birth cohorts corresponding to the nine age groups we used for the 2017-2018
 471 season: 1918-1952, 1953-1967, 1968-1977, 1978-1987, 1988-1997, 1998-2002, 2003-2007, 2008-2012, and 2013-2017. Let
 472 $Q(y)$ be the birth cohort of people born in year y . Then

$$V = V_{s,y} = 1 - v_{Q(y),s},$$

473 where $v_{Q(y),s}$ is the VE among people in cohort $Q(y)$ against infection by dominant subtype s .

474 N2 imprinting

475 We consider that imprinting to N2 reduces a birth cohort's risk of H3N2 infection. Therefore,

$$p_{\text{H3N2},t,y,v} \propto 1 - n_m(m_{\text{H3N2},t,y} + m_{\text{H2N2},t,y}),$$

476 where n_m is the strength of N2 imprinting, and $m_{\text{H3N2},t,y}$ and $m_{\text{H2N2},t,y}$ are the imprinting probabilities of birth cohort y in
477 season t to H3N2 and H2N2.

478 HA subtype imprinting

479 We consider that imprinting to HA reduces a birth cohort's risk of future infection from the same HA subtype. Therefore,

$$p_{s,t,y,v} \propto 1 - h_s m_{s,t,y},$$

480 where h_s is the strength of HA imprinting for subtype s . and $m_{s,t,y}$ is the imprinting probability of birth cohort y in season t to
481 subtype s .

482 HA group imprinting

483 We consider that imprinting to HA reduces a birth cohort's risk of future infection from the viruses within the same HA group.

484 Therefore,

$$p_{\text{H1N1},t,y,v} \propto 1 - g_1(m_{\text{H1N1},t,y} + m_{\text{H2N2},t,y}),$$

$$p_{\text{H3N2},t,y,v} \propto 1 - g_2 m_{\text{H3N2},t,y},$$

485 where g_1 is the strength of HA imprinting for group 1 viruses and g_2 is the strength of HA imprinting for group 2 viruses.

486 Vaccine imprinting

487 We consider that imprinting via vaccination confers a fraction (x) of the protection conferred by infection. If $x = 0$, vaccination
488 prevents imprinting via infection without protecting against infection in future seasons. If $x = 1$, vaccination imprints as well
489 as infection. Because seasonal vaccines are polyvalent, we assume that imprinting via vaccination protects against both H1N1
490 and H3N2 infections. Imprinting via vaccination by the monovalent pandemic vaccine only protects against H1N1 infections.
491 Therefore, for subtype-specific imprinting,

$$p_{s,t,y,v} \propto 1 - x h_s m_{v,t,y},$$

492 where $m_{v,t,y}$ is the probability of imprinting via vaccination in season t for birth cohort y . Similarly, for group-specific
493 imprinting,

$$p_{\text{H1N1},t,y,v} \propto 1 - x g_1 m_{v,t,y}$$

$$p_{\text{H3N2},t,y,v} \propto 1 - x g_2 m_{v,t,y}.$$

494 In models including vaccine imprinting, the imprinting probabilities for infection differ from the infection-only model.
495 That is, we use the imprinting probabilities from Figure 5-Supplement 3 and not the probabilities from Figure 2. We assume
496 that the protection conferred by imprinting via vaccination cannot exceed protection conferred by initial infection and therefore
497 restrict x to lie between 0 and 1.

498 **Model likelihood**

499 Let $n_{s,t,y,v}$ be the number of PCR-confirmed influenza cases of dominant subtype s in influenza season t among people born in
500 year y with vaccination status v . The total number of PCR-confirmed cases of dominant subtype s in season t is

$$N_{s,t} = \sum_{y=1918}^{y_{\max}} n_{s,t,y,\text{unvac.}} + \sum_{y=1918}^{y_{\max}} n_{s,t,y,\text{vac.}}$$

501 For models fitted to a restricted set of ages, we limited the cases for each season to the birth cohorts that were guaranteed
502 to meet the age requirements in that season.

503 We aim to infer $p_{s,t,y,v}$, the predicted fraction of all PCR-confirmed influenza cases of subtype s in influenza season t
 504 among people born in year y with vaccination status v .

505 For a specific model M , we consider all possible model components j described above (demography, age, vaccination,
 506 and imprinting). Then,

$$p_{s,t,y,v} = k_{M,t} \prod_j M_j,$$

507 where M_j indicates whether model M contains component j (e.g., for HA subtype imprinting, $j = 1 - h_s m_{s,t,y}$).

508 The likelihood for season t is given by the multinomial likelihood,

$$\mathcal{L}_t = \frac{N_{s,t}! p_{s,t,1918,\text{unvac.}}^{n_{s,t,1918,\text{unvac.}}} p_{s,t,1918,\text{vac.}}^{n_{s,t,1918,\text{vac.}}} \cdots p_{s,t,y_{\text{max},t},\text{unvac.}}^{n_{s,t,y_{\text{max},t},\text{unvac.}}} p_{s,t,y_{\text{max},t},\text{vac.}}^{n_{s,t,y_{\text{max},t},\text{vac.}}}}{n_{s,t,1918,\text{unvac.}}! n_{s,t,1918,\text{vac.}}! \cdots n_{s,t,y_{\text{max},t},\text{unvac.}}! n_{s,t,y_{\text{max},t},\text{vac.}}!},$$

509 where $y_{\text{max},t}$ is the maximum birth year possible for a specific season t .

510 The full model likelihood for all observed seasons is

$$\mathcal{L} = \prod_{t=2007-2008}^{2017-2018} \mathcal{L}_t.$$

511 We fitted the model to case data using the L-BFGS-B algorithm implemented in the R package *optimx*. We estimated 95%
 512 confidence intervals for parameters of the best-fitting model by evaluating likelihood profiles at 15 evenly spaced points and
 513 interpolating the entire profile using a smoothing spline.

514 Sensitivity analyses

515 Sensitivity to age groups

516 To test whether our models were sensitive to our choice of age groups, we fit revised versions of all our models with different
 517 age groups:

- 518 • 0-4 years, 5-17 years, 18-49 years, 50-64 years, and ≥ 65 years
- 519 • 0-4 years, 5-17 years, 18-64 years, and ≥ 65 years

520 These models with alternate age groupings were fitted to case data to determine whether our findings on the strength of
 521 protection from initial H1N1 and H3N2 infection significantly changed from our fits using the higher-resolution age grouping
 522 described above (Appendix 1 Table 3).

523 Sensitivity to sampling effort

524 Sampling effort was not even across seasons, and analysis of the number of influenza cases per sampling day suggested that a
 525 significant number of cases may have been missed at the beginning or end of a specific seasons (Figure 5-Supplement 1). As
 526 our analysis of relative risk indicates, different age groups are more susceptible during different points in the influenza season,
 527 and therefore missing data from the beginning or end of a season could introduce bias in the observed age distribution of
 528 cases.

529 To adjust for this, we simulated cases for seasons which did not have sufficient sampling of the start or end of the epidemic
 530 period. We considered a season sufficiently sampled if

- 531 • the number of cases per sampling day in the first week of the enrollment period was < 1 and
- 532 • the number of cases per sampling day in the last week of the enrollment period was < 1 .

533 To extrapolate the start of a season, we linearly regressed the number of cases of the dominant subtype per sampling day
 534 for each week of the first half of the season and identified the week of the season where the number of cases per sampling
 535 day fell below 1 (t_0). For each week from t_0 to the first week of the enrollment period, we used the regression of cases per
 536 sampling day to calculate the number of cases we expected to see in each week. Summing these yields the total number of
 537 unsampled cases at the beginning of the season. We used a similar approach to extrapolate the number of unsampled cases at
 538 the end of a season by instead regressing cases per sampling day for each week of the latter half of the season. We did not
 539 extrapolate cases for the 2010-2011 season for this analysis since the observed number of cases per sampling day did not
 540 follow a typical epidemic curve.

541 We stochastically assigned a birth year and vaccination status to these cases according to a multinomial distribution. The
542 success probabilities of this distribution were set using the age distribution of cases of the dominant subtype from the first two
543 weeks of the enrollment period (if extrapolating the beginning of a season) or the last two weeks of the enrollment period (if
544 extrapolating the end of a season). Specifically, we calculated the distribution of observed cases in the first or last two weeks
545 of the enrollment period among nine age groups (described above in "Age-specific factors") with their associated vaccination
546 status. We then assumed that cases were uniformly distributed among all birth years contained in an age group. This yielded
547 a set of probabilities describing the probability of infection given birth year and vaccination status in a specific season.

548 We sampled from these multinomial distributions 1000 times to obtain augmented datasets that combined observed and
549 extrapolated cases. For each replicate simulation, we calculated the age distribution of cases for the entire season as well as
550 the relative risk of each age group in the first versus the latter half of the season (Figure 1-Supplement 2B). We also fitted the
551 best-fitting model to 100 of these datasets (excluding the 2010-2011 season) and recorded the estimated imprinting strength
552 for both H1N1 and H3N2 for each fit (Figure 5-Supplement 2).

553 **Calculating excess cases**

554 We defined excess cases for a given birth cohort or age group as the number of observed cases for that birth cohort or age group
555 minus the number of predicted cases for that age group. Predictions were obtained by multiplying the multinomial probabilities
556 produced by the model by the total number of cases of the dominant subtype in each season. A 95% prediction interval
557 was obtained by simulating 100 datasets using the multinomial probabilities from a specific model (Figure 6-Supplement 2,
558 Figure 7).

559 To test whether recent infection might be confounding our estimates, we calculated the correlation between excess cases
560 in each birth cohort in each season with excess cases of the same birth cohort in the next season with the same dominant
561 subtype (Figure 5-Supplement 5).

562 **Code and data availability**

563 The code and data used to perform the analyses for this project are available at <https://github.com/cobeylab/FluAImprinting>.

564 **Ethics**

565 Human subjects: Study procedures for the vaccine effectiveness study was approved by the IRB at the Marshfield Clinic
566 Research Institute. Informed consent was obtained from all participants at the time of enrollment into the vaccine effectiveness
567 study. This analysis was subsequently approved by the IRB with a waiver of informed consent. The analysis of data was
568 approved by the University of Chicago IRB.

569 **Acknowledgments**

570 We thank Jennifer King and Carla Rottscheit for their assistance in providing the data for this study and Rohan Dandavati for
571 compiling historical data on subtype frequencies and ILI. We thank Marcos Vieira and Kangchon Kim for their assistance
572 in calculating imprinting probabilities. We also thank the study participants for their time. This work was completed with
573 computational resources provided by the University of Chicago's Research Computing Center. Funding for this project was
574 provided by the National Institutes of Health (NIH), Department of Health and Human Services, under grant DP2AI117921
575 (to SC) and CEIRS Contract No. HHSN272201400005C (to SC). HQM receives research support from Seqirus unrelated to
576 this work. The funders had no role in study design, data collection and analysis, decision to publish, or preparation of the
577 manuscript.

578 **References**

- 579 **Ann J**, Papenburg J, Bouhy X, Rheaume C, Hamelin ME, Boivin G. Molecular and antigenic evolution of human influenza A/H3N2 viruses
580 in Quebec, Canada, 2009-2011. *J Clin Virol.* 2012; 53(1):88-92. doi: 10.1016/j.jcv.2011.09.016.
- 581 **Arriola CS**, Brammer L, Epperson S, Blanton L, Kniss K, Mustaquim D, Steffens C, Dhara R, Leon M, Perez A, Chaves SS, Katz J, Wallis T,
582 Villanueva J, Xu X, Abd Elal AI, Gubareva L, Cox N, Finelli L, Bresee J, et al. Update: influenza activity - United States, September 29,
583 2013-February 8, 2014. *MMWR Morbidity and mortality weekly report.* 2014; 63(7):148-154. <https://www.ncbi.nlm.nih.gov/pubmed/24553198>
584 <https://www.ncbi.nlm.nih.gov/pmc/PMC4584759/>.

- 585 **Beauté J**, Zucs P, Korsun N, Bragstad K, Enouf V, Kossyvakis A, Griškevičius A, Olinger CM, Meijer A, Guimar R, Prosenc K, Staroňová E,
586 Delgado C, Brytting M, Broberg E, European Influenza Surveillance N. Age-specific differences in influenza virus type and subtype distri-
587 bution in the 2012/2013 season in 12 European countries. *Epidemiology and Infection*. 2015; 143(14):2950–2958. <https://www.ncbi.nlm.nih.gov/pubmed/25648399><https://www.ncbi.nlm.nih.gov/pmc/PMC4595855/>, doi: 10.1017/S0950268814003422.
- 589 **Bedford T**, Riley S, Barr IG, Broor S, Chadha M, Cox NJ, Daniels RS, Gunasekaran CP, Hurt AC, Kelso A, Klimov A, Lewis NS, Li X,
590 McCauley JW, Odagiri T, Potdar V, Rambaut A, Shu Y, Skepner E, Smith DJ, et al. Global circulation patterns of seasonal influenza
591 viruses vary with antigenic drift. *Nature*. 2015; 523:217. <https://doi.org/10.1038/nature14460>, doi: 10.1038/nature14460.
- 592 **Belongia EA**, Kieke BA, Donahue JG, Coleman LA, Irving SA, Meece JK, Vandermause M, Lindstrom S, Gargiullo P, Shay DK. Influenza
593 vaccine effectiveness in Wisconsin during the 2007–08 season: comparison of interim and final results. *Vaccine*. 2011; 29(38):6558–63.
594 doi: 10.1016/j.vaccine.2011.07.002.
- 595 **Belongia EA**, Kieke BA, Donahue JG, Greenlee RT, Balish A, Foust A, Lindstrom S, Shay DK. Effectiveness of Inactivated Influenza
596 Vaccines Varied Substantially with Antigenic Match from the 2004–2005 Season to the 2006–2007 Season. *The Journal of Infectious
597 Diseases*. 2009; 199(2):159–167. <https://doi.org/10.1086/595861>, doi: 10.1086/595861.
- 598 **Biggerstaff M**, Jhung MA, Reed C, Fry AM, Balluz L, Finelli L. Influenza-like illness, the time to seek healthcare, and influenza antiviral
599 receipt during the 2010–2011 influenza season—United States. *The Journal of infectious diseases*. 2014; 210(4):535–544.
- 600 **Bodewes R**, de Mutsert G, van der Klis FRM, Ventresca M, Wilks S, Smith DJ, Koopmans M, Fouchier RAM, Osterhaus ADME, Rimmelzwaan
601 GF. Prevalence of Antibodies against Seasonal Influenza A and B Viruses in Children in Netherlands. *Clinical and Vaccine Immunology*.
602 2011; 18(3):469–476. <https://cvi.asm.org/content/cdli/18/3/469.full.pdf>, doi: 10.1128/cvi.00396-10.
- 603 **Bridges CB**, Fukuda K, Uyeki TM, Cox NJ, Singleton JA. Prevention and control of influenza. Recommendations of the Advisory Committee
604 on Immunization Practices (ACIP). *MMWR Recomm Rep*. 2002; 51(Rr-3):1–31.
- 605 **Brooks-Pollock E**, Tilston N, Edmunds WJ, Eames KTD. Using an online survey of healthcare-seeking behaviour to estimate the magnitude
606 and severity of the 2009 H1N1v influenza epidemic in England. *BMC Infectious Diseases*. 2011; 11(1):68. <https://doi.org/10.1186/1471-2334-11-68>,
607 doi: 10.1186/1471-2334-11-68.
- 608 **Budd AP**, Beacham L, Smith CB, Garten RJ, Reed C, Kniss K, Mustaqim D, Ahmad FB, Cummings CN, Garg S, Levine MZ, Fry AM,
609 Brammer L. Birth Cohort Effects in Influenza Surveillance Data: Evidence that First Influenza Infection Affects Later Influenza-Associated
610 Illness. *The Journal of Infectious Diseases*. 2019; <https://doi.org/10.1093/infdis/jiz201>, doi: 10.1093/infdis/jiz201.
- 611 **Caini S**, Spreuuenberg P, Kuszniierz GF, Rudi JM, Owen R, Pennington K, Wangchuk S, Gyeltshen S, Ferreira de Almeida WA, Pessanha Hen-
612 riques CM, Njouom R, Vernet MA, Fasce RA, Andrade W, Yu H, Feng L, Yang J, Peng Z, Lara J, Bruno A, et al. Distribution of influenza
613 virus types by age using case-based global surveillance data from twenty-nine countries, 1999–2014. *BMC infectious diseases*. 2018;
614 18(1):269–269. <https://www.ncbi.nlm.nih.gov/pubmed/29884140><https://www.ncbi.nlm.nih.gov/pmc/PMC5994061/>,
615 doi: 10.1186/s12879-018-3181-y.
- 616 **CDC**, FluView National, Regional, and State Level Outpatient Illness and Viral Surveillance. Accessed 23-October-2018; 2018. <https://gis.cdc.gov/grasp/fluview/fluportaldashboard.html>.
617
- 618 **CMS**, Nursing Home Compendium 2015 Edition. Accessed 30-September-2019; 2015. [https://www.cms.gov/Medicare/
619 Provider-Enrollment-and-Certification/CertificationandCompliance/downloads/nursinghomedatacompendium_
620 508-2015.pdf](https://www.cms.gov/Medicare/Provider-Enrollment-and-Certification/CertificationandCompliance/downloads/nursinghomedatacompendium_508-2015.pdf).
- 621 **Cobey S**, Koelle K. Capturing escape in infectious disease dynamics. *Trends Ecol Evol*. 2008; 23(10):572–7. doi: 10.1016/j.tree.2008.06.008.
- 622 **Cobey S**, Hensley SE. Immune history and influenza virus susceptibility. *Current Opinion in Virology*. 2017; 22:105–111. <http://www.sciencedirect.com/science/article/pii/S1879625716302127>, doi: <https://doi.org/10.1016/j.coviro.2016.12.004>.
- 624 **Davenport FM**, Hennessy AV. A serologic recapitulation of past experiences with influenza A; antibody response to monovalent vaccine,
625 vol. 104; 1956. doi: 10.1084/jem.104.1.85.
- 626 **Davenport FM**, Hennessy AV. Predetermination by infection and by vaccination of antibody response to influenza virus vaccines. *J Exp
627 Med*. 1957; 106(6):835–50. doi: 10.1084/jem.106.6.835.
- 628 **Davis AKF**, McCormick K, Gumina ME, Petrie JG, Martin ET, Xue KS, Bloom JD, Monto AS, Bushman FD, Hensley SE. Sera from
629 Individuals with Narrowly Focused Influenza Virus Antibodies Rapidly Select Viral Escape Mutations In Ovo. *Journal of Virology*. 2018;
630 92(19). <https://jvi.asm.org/content/92/19/e00859-18>, doi: 10.1128/JVI.00859-18.
- 631 **DiazGranados CA**, Dunning AJ, Kimmel M, Kirby D, Treanor J, Collins A, Pollak R, Christoff J, Earl J, Landolfi V. Efficacy of high-dose
632 versus standard-dose influenza vaccine in older adults. *New England Journal of Medicine*. 2014; 371(7):635–645.

- 633 **Dávila J**, Chowell G, Borja-Aburto VH, Viboud C, Grajales Muñiz C, Miller M. Substantial Morbidity and Mortality Associated
634 with Pandemic A/H1N1 Influenza in Mexico, Winter 2013-2014: Gradual Age Shift and Severity. *PLoS currents*. 2014; 6:cur-
635 rents.outbreaks.a855a92f19db1d90ca955f5e908d6631. <https://www.ncbi.nlm.nih.gov/pubmed/24744975><https://www.ncbi.nlm.nih.gov/pmc/PMC3967911/>, doi: 10.1371/currents.outbreaks.a855a92f19db1d90ca955f5e908d6631.
- 637 **Englund JA**, Walter EB, Fairchok MP, Monto AS, Neuzil KM. A comparison of 2 influenza vaccine schedules in 6- to 23-month-old children.
638 *Pediatrics*. 2005; 115(4):1039–47. doi: 10.1542/peds.2004-2373.
- 639 **Erbelding EJ**, Post DJ, Stemmy EJ, Roberts PC, Augustine AD, Ferguson S, Paules CI, Graham BS, Fauci AS. A Universal Influenza
640 Vaccine: The Strategic Plan for the National Institute of Allergy and Infectious Diseases. *The Journal of Infectious Diseases*. 2018 02;
641 218(3):347–354. <https://doi.org/10.1093/infdis/jiy103>, doi: 10.1093/infdis/jiy103.
- 642 **Flannery B**, Smith C, Garten RJ, Levine MZ, Chung JR, Jackson ML, Jackson LA, Monto AS, Martin ET, Belongia EA, McLean HQ,
643 Gaglani M, Murthy K, Zimmerman R, Nowalk MP, Griffin MR, Keipp Talbot H, Treanor JJ, Wentworth DE, Fry AM. Influence of Birth
644 Cohort on Effectiveness of 2015-2016 Influenza Vaccine Against Medically Attended Illness Due to 2009 Pandemic Influenza A(H1N1)
645 Virus in the United States. *J Infect Dis*. 2018; 218(2):189–196. doi: 10.1093/infdis/jix634.
- 646 **Fonville JM**, Fraaij PLA, de Mutsert G, Wilks SH, van Beek R, Fouchier RAM, Rimmelzwaan GF. Antigenic Maps of Influenza A(H3N2)
647 Produced With Human Antisera Obtained After Primary Infection. *The Journal of Infectious Diseases*. 2015; 213(1):31–38. <https://doi.org/10.1093/infdis/jiv367>, doi: 10.1093/infdis/jiv367.
- 649 **Francis T**. On the doctrine of original antigenic sin. *Proceedings of the American Philosophical Society*. 1960; 104(6):572–578.
- 650 **Gaglani M**, Pruszynski J, Murthy K, Clipper L, Robertson A, Reis M, Chung JR, Piedra PA, Avadhanula V, Nowalk MP, Zimmerman
651 RK, Jackson ML, Jackson LA, Petrie JG, Ohmit SE, Monto AS, McLean HQ, Belongia EA, Fry AM, Flannery B. Influenza Vaccine
652 Effectiveness Against 2009 Pandemic Influenza A(H1N1) Virus Differed by Vaccine Type During 2013-2014 in the United States. *J Infect*
653 *Dis*. 2016; 213(10):1546–56. doi: 10.1093/infdis/jiv577.
- 654 **Gagnon A**, Acosta E, Hallman S, Bourbeau R, Dillon LY, Ouellette N, Earn DJD, Herring DA, Inwood K, Madrenas J, Miller MS. Pandemic
655 Paradox: Early Life H2N2 Pandemic Influenza Infection Enhanced Susceptibility to Death during the 2009 H1N1 Pandemic. *mBio*. 2018;
656 9(1):e02091–17. <https://mbio.asm.org/content/mbio/9/1/e02091-17.full.pdf>, doi: 10.1128/mBio.02091-17.
- 657 **Gagnon A**, Miller MS, Hallman SA, Bourbeau R, Herring DA, Earn DJD, Madrenas J. Age-Specific Mortality During the 1918 Influenza
658 Pandemic: Unravelling the Mystery of High Young Adult Mortality. *PLOS ONE*. 2013; 8(8):e69586. [https://doi.org/10.1371/](https://doi.org/10.1371/journal.pone.0069586)
659 [journal.pone.0069586](https://doi.org/10.1371/journal.pone.0069586), doi: 10.1371/journal.pone.0069586.
- 660 **Goldstein E**, Cobey S, Takahashi S, Miller JC, Lipsitch M. Predicting the Epidemic Sizes of Influenza A/H1N1, A/H3N2, and B: A
661 Statistical Method. *PLOS Medicine*. 2011; 8(7):e1001051. <https://doi.org/10.1371/journal.pmed.1001051>, doi: 10.1371/jour-
662 [nal.pmed.1001051](https://doi.org/10.1371/journal.pmed.1001051).
- 663 **Gostic KM**, Ambrose M, Worobey M, Lloyd-Smith JO. Potent protection against H5N1 and H7N9 influenza via childhood hemagglutinin
664 imprinting. *Science*. 2016; 354(6313):722–726. doi: 10.1126/science.aag1322.
- 665 **Griffin MR**, Monto AS, Belongia EA, Treanor JJ, Chen Q, Chen J, Talbot HK, Ohmit SE, Coleman LA, Lofthus G, Petrie JG, Meece JK, Hall
666 CB, Williams JV, Gargiullo P, Berman L, Shay DK. Effectiveness of non-adjuvanted pandemic influenza A vaccines for preventing pandemic
667 influenza acute respiratory illness visits in 4 U.S. communities. *PLoS One*. 2011; 6(8):e23085. doi: 10.1371/journal.pone.0023085.
- 668 **Groth SFdS**, Webster R. Disquisitions on original antigenic sin: I. Evidence in man. *Journal of Experimental Medicine*. 1966; 124(3):331–
669 345.
- 670 **Huang KYA**, Rijal P, Schimanski L, Powell TJ, Lin TY, McCauley JW, Daniels RS, Townsend AR. Focused antibody response to influenza
671 linked to antigenic drift. *The Journal of clinical investigation*. 2015; 125(7):2631–2645.
- 672 **Huang QS**, Bandaranayake D, Wood T, Newbern EC, Seeds R, Ralston J, Waite B, Bissielo A, Prasad N, Todd A, Jelley L, Gunn W,
673 McNicholas A, Metz T, Lawrence S, Collis E, Retter A, Wong SS, Webby R, Bocacao J, et al. Risk Factors and Attack Rates of Seasonal
674 Influenza Infection: Results of the Southern Hemisphere Influenza and Vaccine Effectiveness Research and Surveillance (SHIVERS)
675 Seroepidemiologic Cohort Study. *J Infect Dis*. 2019; 219(3):347–357. doi: 10.1093/infdis/jiy443.
- 676 **Irving SA**, Donahue JG, Shay DK, Ellis-Coyle TL, Belongia EA. Evaluation of self-reported and registry-based influenza vaccination status
677 in a Wisconsin cohort. *Vaccine*. 2009; 27(47):6546–9. doi: 10.1016/j.vaccine.2009.08.050.
- 678 **Jackson LA**, Jackson ML, Nelson JC, Neuzil KM, Weiss NS. Evidence of bias in estimates of influenza vaccine effectiveness in seniors.
679 *International Journal of Epidemiology*. 2005 12; 35(2):337–344. <https://doi.org/10.1093/ije/dyi274>, doi: 10.1093/ije/dyi274.
- 680 **Jackson LA**, Nelson JC, Benson P, Neuzil KM, Reid RJ, Psaty BM, Heckbert SR, Larson EB, Weiss NS. Functional status is a confounder
681 of the association of influenza vaccine and risk of all cause mortality in seniors. *International Journal of Epidemiology*. 2005 12;
682 35(2):345–352. <https://doi.org/10.1093/ije/dyi275>, doi: 10.1093/ije/dyi275.

- 683 **Jackson ML**, Chung JR, Jackson LA, Phillips CH, Benoit J, Monto AS, Martin ET, Belongia EA, McLean HQ, Gaglani M, Murthy K,
684 Zimmerman R, Nowalk MP, Fry AM, Flannery B. Influenza Vaccine Effectiveness in the United States during the 2015-2016 Season. *N*
685 *Engl J Med.* 2017; 377(6):534–543. doi: 10.1056/NEJMoa1700153.
- 686 **Khiabanian H**, Farrell GM, St George K, Rabadan R. Differences in patient age distribution between influenza A subtypes. *PLoS*
687 *one.* 2009; 4(8):e6832–e6832. <https://www.ncbi.nlm.nih.gov/pubmed/19718262>[https://www.ncbi.nlm.nih.gov/pmc/](https://www.ncbi.nlm.nih.gov/pmc/PMC2729409/)
688 [PMC2729409/](https://www.ncbi.nlm.nih.gov/pmc/PMC2729409/), doi: 10.1371/journal.pone.0006832.
- 689 **Kieke AL**, Kieke BA, Kopitzke SL, McClure DL, Belongia EA, VanWormer JJ, Greenlee RT. Validation of Health Event Capture in
690 the Marshfield Epidemiologic Study Area. *Clinical Medicine & Research.* 2015; 13(3-4):103–111. [http://www.clinmedres.org/](http://www.clinmedres.org/content/13/3-4/103.abstract)
691 [content/13/3-4/103.abstract](http://www.clinmedres.org/content/13/3-4/103.abstract), doi: 10.3121/cmr.2014.1246.
- 692 **Laurie KL**, Guarnaccia TA, Carolan LA, Yan AWC, Aban M, Petrie S, Cao P, Heffernan JM, McVernon J, Mosse J, Kelso A, McCaw JM, Barr
693 IG. Interval Between Infections and Viral Hierarchy Are Determinants of Viral Interference Following Influenza Virus Infection in a Ferret
694 Model. *The Journal of infectious diseases.* 2015; 212(11):1701–1710. <https://www.ncbi.nlm.nih.gov/pubmed/25943206>[https://www.ncbi.nlm.nih.gov/pmc/](https://www.ncbi.nlm.nih.gov/pmc/PMC4633756/)
695 [PMC4633756/](https://www.ncbi.nlm.nih.gov/pmc/PMC4633756/), doi: 10.1093/infdis/jiv260.
- 696 **Lee JKH**, Lam GKL, Shin T, Kim J, Krishnan A, Greenberg DP, Chit A. Efficacy and effectiveness of high-dose versus standard-dose
697 influenza vaccination for older adults: a systematic review and meta-analysis. *Expert Review of Vaccines.* 2018; 17(5):435–443.
698 <https://doi.org/10.1080/14760584.2018.1471989>, doi: 10.1080/14760584.2018.1471989.
- 699 **Lee JM**, Eguia R, Zost SJ, Choudhary S, Wilson PC, Bedford T, Stevens-Ayers T, Boeckh M, Hurt A, Lakdawala SS, Hensley SE, Bloom JD.
700 Mapping person-to-person variation in viral mutations that escape polyclonal serum targeting influenza hemagglutinin. *bioRxiv.* 2019;
701 <https://www.biorxiv.org/content/early/2019/06/13/670497>, doi: 10.1101/670497.
- 702 **Lewnard JA**, Tedijanto C, Cowling BJ, Lipsitch M. Measurement of Vaccine Direct Effects Under the Test-Negative Design. *American*
703 *Journal of Epidemiology.* 2018 08; 187(12):2686–2697. <https://doi.org/10.1093/aje/kwy163>, doi: 10.1093/aje/kwy163.
- 704 **Linderman SL**, Chambers BS, Zost SJ, Parkhouse K, Li Y, Herrmann C, Ellebedy AH, Carter DM, Andrews SF, Zheng NY, Huang M, Huang
705 Y, Strauss D, Shaz BH, Hodinka RL, Reyes-Terán G, Ross TM, Wilson PC, Ahmed R, Bloom JD, et al. Potential antigenic explanation for
706 atypical H1N1 infections among middle-aged adults during the 2013–2014 influenza season. *Proceedings of the National Academy of*
707 *Sciences.* 2014; 111(44):15798. <http://www.pnas.org/content/111/44/15798.abstract>, doi: 10.1073/pnas.1409171111.
- 708 **Manicassamy B**, Medina RA, Hai R, Tsibane T, Stertz S, Nistal-Villán E, Palese P, Basler CF, García-Sastre A. Protection of mice against
709 lethal challenge with 2009 H1N1 influenza A virus by 1918-like and classical swine H1N1 based vaccines. *PLoS pathogens.* 2010;
710 6(1):e1000745.
- 711 **McLean HQ**, Thompson MG, Sundaram ME, Kieke BA, Gaglani M, Murthy K, Piedra PA, Zimmerman RK, Nowalk MP, Raviotta JM,
712 Jackson ML, Jackson L, Ohmit SE, Petrie JG, Monto AS, Meece JK, Thaker SN, Clippard JR, Spencer SM, Fry AM, et al. Influenza
713 Vaccine Effectiveness in the United States During 2012–2013: Variable Protection by Age and Virus Type. *The Journal of Infectious*
714 *Diseases.* 2014 11; 211(10):1529–1540. <https://doi.org/10.1093/infdis/jiu647>, doi: 10.1093/infdis/jiu647.
- 715 **McLean HQ**, Thompson MG, Sundaram ME, Meece JK, McClure DL, Friedrich TC, Belongia EA. Impact of repeated vaccination on
716 vaccine effectiveness against influenza A (H3N2) and B during 8 seasons. *Clinical Infectious Diseases.* 2014; 59(10):1375–1385.
- 717 **Monto AS**, Koopman JS, Longini J I M. Tecumseh study of illness. XIII. Influenza infection and disease, 1976-1981. *Am J Epidemiol.* 1985;
718 121(6):811–22. doi: 10.1093/oxfordjournals.aje.a114052.
- 719 **Neuzil KM**, Jackson LA, Nelson J, Klimov A, Cox N, Bridges CB, Dunn J, DeStefano F, Shay D. Immunogenicity and Reactogenicity of 1
720 versus 2 Doses of Trivalent Inactivated Influenza Vaccine in Vaccine-Naive 5–8-Year-Old Children. *The Journal of Infectious Diseases.*
721 2006; 194(8):1032–1039. <https://doi.org/10.1086/507309>, doi: 10.1086/507309.
- 722 **O'Donnell CD**, Wright A, Vogel LN, Wei CJ, Nabel GJ, Subbarao K. Effect of Priming with H1N1 Influenza Viruses of Variable Antigenic
723 Distances on Challenge with 2009 Pandemic H1N1 Virus. *Journal of Virology.* 2012; 86(16):8625–8633. [https://jvi.asm.org/](https://jvi.asm.org/content/jvi/86/16/8625.full.pdf)
724 [content/jvi/86/16/8625.full.pdf](https://jvi.asm.org/content/jvi/86/16/8625.full.pdf), doi: 10.1128/jvi.00147-12.
- 725 **Ohmit SE**, Thompson MG, Petrie JG, Thaker SN, Jackson ML, Belongia EA, Zimmerman RK, Gaglani M, Lamerato L, Spencer SM,
726 Jackson L, Meece JK, Nowalk MP, Song J, Zervos M, Cheng PY, Rinaldo CR, Clipper L, Shay DK, Piedra P, et al. Influenza vaccine
727 effectiveness in the 2011-2012 season: protection against each circulating virus and the effect of prior vaccination on estimates. *Clin*
728 *Infect Dis.* 2014; 58(3):319–27. doi: 10.1093/cid/cit736.
- 729 **Petrie JG**, Parkhouse K, Ohmit SE, Malosh RE, Monto AS, Hensley SE. Antibodies Against the Current Influenza A(H1N1) Vaccine
730 Strain Do Not Protect Some Individuals From Infection With Contemporary Circulating Influenza A(H1N1) Virus Strains. *The Journal*
731 *of infectious diseases.* 2016; 214(12):1947–1951. <https://www.ncbi.nlm.nih.gov/pubmed/27923954>[https://www.ncbi.nlm.nih.gov/pmc/](https://www.ncbi.nlm.nih.gov/pmc/PMC5142093/)
732 [PMC5142093/](https://www.ncbi.nlm.nih.gov/pmc/PMC5142093/), doi: 10.1093/infdis/jiw479.

- 733 **Ranjeva S**, Subramanian R, Fang VJ, Leung GM, Ip DKM, Perera RAPM, Peiris JSM, Cowling BJ, Cobey S. Age-specific differences
734 in the dynamics of protective immunity to influenza. *Nature Communications*. 2019; 10(1):1660. <https://doi.org/10.1038/s41467-019-09652-6>, doi: 10.1038/s41467-019-09652-6.
- 736 **Reed C**, Chaves SS, Daily Kirley P, Emerson R, Aragon D, Hancock EB, Butler L, Baumbach J, Hollick G, Bennett NM, Laidler MR,
737 Thomas A, Meltzer MI, Finelli L. Estimating influenza disease burden from population-based surveillance data in the United States. *PLoS*
738 *One*. 2015; 10(3):e0118369. doi: 10.1371/journal.pone.0118369.
- 739 **Saito N**, Komori K, Suzuki M, Kishikawa T, Yasaka T, Ariyoshi K. Dose-Dependent Negative Effects of Prior Multiple Vaccinations Against
740 Influenza A and Influenza B Among Schoolchildren: A Study of Kamigoto Island in Japan During the 2011–2012, 2012–2013, and
741 2013–2014 Influenza Seasons. *Clinical Infectious Diseases*. 2018; 67(6):897–904.
- 742 **Santibanez TA**, Lu PJ, O'Halloran A, Meghani A, Grabowsky M, Singleton JA. Trends in Childhood Influenza Vaccination Coverage—U.S.,
743 2004–2012. *Public Health Reports*. 2014; 129(5):417–427. doi: 10.1177/003335491412900505, PMID: 25177053.
- 744 **Santibanez TA**, Santoli JM, Bridges CB, Euler GL. Influenza Vaccination Coverage of Children Aged 6 to 23 Months: The 2002–2003 and
745 2003–2004 Influenza Seasons. *Pediatrics*. 2006; 118(3):1167–1175. [https://pediatrics.aappublications.org/content/118/](https://pediatrics.aappublications.org/content/118/3/1167)
746 [3/1167](https://pediatrics.aappublications.org/content/118/3/1167), doi: 10.1542/peds.2006-0831.
- 747 **Skowronski DM**, Chambers C, De Serres G, Sabaiduc S, Winter AL, Dickinson JA, Gubbay JB, Fonseca K, Drews SJ, Charest H, Martineau
748 C, Krajdén M, Petric M, Bastien N, Li Y, Smith DJ. Serial Vaccination and the Antigenic Distance Hypothesis: Effects on Influenza
749 Vaccine Effectiveness During A(H3N2) Epidemics in Canada, 2010–2011 to 2014–2015. *J Infect Dis*. 2017; 215(7):1059–1099. doi:
750 10.1093/infdis/jix074.
- 751 **Skowronski DM**, Chambers C, Sabaiduc S, De Serres G, Winter AL, Dickinson JA, Gubbay JB, Drews SJ, Martineau C, Charest H, Krajdén
752 M, Bastien N, Li Y. Beyond Antigenic Match: Possible Agent-Host and Immuno-epidemiological Influences on Influenza Vaccine
753 Effectiveness During the 2015–2016 Season in Canada. *J Infect Dis*. 2017; 216(12):1487–1500. doi: 10.1093/infdis/jix526.
- 754 **Skowronski DM**, Chambers C, Sabaiduc S, De Serres G, Winter AL, Dickinson JA, Krajdén M, Gubbay JB, Drews SJ, Martineau C, et al. A
755 perfect storm: impact of genomic variation and serial vaccination on low influenza vaccine effectiveness during the 2014–2015 season.
756 *Clinical Infectious Diseases*. 2016; 63(1):21–32.
- 757 **Smith DJ**, Lapedes AS, de Jong JC, Bestebroer TM, Rimmelzwaan GF, Osterhaus AD, Fouchier RA. Mapping the antigenic and genetic
758 evolution of influenza virus. *Science*. 2004; 305(5682):371–6. doi: 10.1126/science.1097211.
- 759 **Smith DJ**, Forrest S, Ackley DH, Perelson AS. Variable efficacy of repeated annual influenza vaccination. *Proceedings of the National*
760 *Academy of Sciences*. 1999; 96(24):14001–14006. <https://www.pnas.org/content/96/24/14001>, doi: 10.1073/pnas.96.24.14001.
- 761 **Sullivan SG**, Tchetchen Tchetchen EJ, Cowling BJ. Theoretical Basis of the Test-Negative Study Design for Assessment of Influenza
762 Vaccine Effectiveness. *American journal of epidemiology*. 2016; 184(5):345–353. [https://www.ncbi.nlm.nih.gov/pubmed/](https://www.ncbi.nlm.nih.gov/pubmed/27587721)
763 [27587721](https://www.ncbi.nlm.nih.gov/pubmed/27587721)<https://www.ncbi.nlm.nih.gov/pmc/PMC5013887/>, doi: 10.1093/aje/kww064.
- 764 **Thompson WW**, Shay DK, Weintraub E, Brammer L, Cox N, Anderson LJ, Fukuda K. Mortality Associated With Influenza and Res-
765 piratory Syncytial Virus in the United States. *JAMA*. 2003; 289(2):179–186. <https://doi.org/10.1001/jama.289.2.179>, doi:
766 10.1001/jama.289.2.179.
- 767 **Treanor JJ**, Talbot HK, Ohmit SE, Coleman LA, Thompson MG, Cheng PY, Petrie JG, Lofthus G, Meece JK, Williams JV, Berman L,
768 Breese Hall C, Monto AS, Griffin MR, Belongia E, Shay DK. Effectiveness of seasonal influenza vaccines in the United States during a
769 season with circulation of all three vaccine strains. *Clin Infect Dis*. 2012; 55(7):951–9. doi: 10.1093/cid/cis574.
- 770 **Van Caunteren D**, Vaux S, de Valk H, Le Strat Y, Vaillant V, Lévy-Bruhl D. Burden of influenza, healthcare seeking behaviour and
771 hygiene measures during the A(H1N1)2009 pandemic in France: a population based study. *BMC Public Health*. 2012; 12(1):947.
772 <https://doi.org/10.1186/1471-2458-12-947>, doi: 10.1186/1471-2458-12-947.
- 773 **WDHS**, Nursing Home Directory. Accessed 30-September-2019; 2018. [https://www.dhs.wisconsin.gov/guide/nursing-home.](https://www.dhs.wisconsin.gov/guide/nursing-home.htm)
774 [htm](https://www.dhs.wisconsin.gov/guide/nursing-home.htm).
- 775 **Worby CJ**, Chaves SS, Wallinga J, Lipsitch M, Finelli L, Goldstein E. On the relative role of different age groups in influenza epi-
776 demics. *Epidemics*. 2015; 13:10–16. <https://www.ncbi.nlm.nih.gov/pubmed/26097505><https://www.ncbi.nlm.nih.gov/pmc/PMC4469206/>, doi: 10.1016/j.epidem.2015.04.003.
- 778 **Worobey M**, Han GZ, Rambaut A. Genesis and pathogenesis of the 1918 pandemic H1N1 influenza A virus. *Proceedings of the National*
779 *Academy of Sciences of the United States of America*. 2014; 111(22):8107–8112. [https://www.ncbi.nlm.nih.gov/pubmed/](https://www.ncbi.nlm.nih.gov/pubmed/24778238)
780 [24778238](https://www.ncbi.nlm.nih.gov/pubmed/24778238)<https://www.ncbi.nlm.nih.gov/pmc/PMC4050607/>, doi: 10.1073/pnas.1324197111.

- 781 **Wu JT**, Ma ES, Lee CK, Chu DK, Ho PL, Shen AL, Ho A, Hung IF, Riley S, Ho LM, Lin CK, Tsang T, Lo SV, Lau YL, Leung GM,
782 Cowling BJ, Malik Peiris JS. The infection attack rate and severity of 2009 pandemic H1N1 influenza in Hong Kong. *Clin Infect Dis*.
783 2010; 51(10):1184–91. doi: 10.1086/656740.
- 784 **Wu S**, L VANA, Wang L, McDonald SA, Pan Y, Duan W, Zhang L, Sun Y, Zhang Y, Zhang X, Pilot E, Krafft T, W VDH, MAB VDS, Yang
785 P, Wang Q. Estimated incidence and number of outpatient visits for seasonal influenza in 2015–2016 in Beijing, China. *Epidemiology and*
786 *infection*. 2017; 145(16):3334–3344. doi: 10.1017/s0950268817002369.
- 787 **Zimmerman RK**, Nowalk MP, Chung J, Jackson ML, Jackson LA, Petrie JG, Monto AS, McLean HQ, Belongia EA, Gaglani M, Murthy K,
788 Fry AM, Flannery B, Investigators ftUFV. 2014–2015 Influenza Vaccine Effectiveness in the United States by Vaccine Type. *Clinical*
789 *Infectious Diseases*. 2016; 63(12):1564–1573. <https://doi.org/10.1093/cid/ciw635>, doi: 10.1093/cid/ciw635.

790 **Supplementary tables and figures**

Appendix 1 Table 1. Estimates of parameters shared by the age-specific VE and birth-cohort-specific VE models.

	Model with ge-specific VE, age ≥ 6 months (MLE 95% CI)	Model with age-specific VE, age ≥ 10 years (MLE, 95% CI)	Model with age-specific VE, age <65 years (MLE, 95% CI)	Model with age-specific VE, age 10-64 years (MLE, 95% CI)	Model with birth-cohort-specific VE, age ≥ 10 years (MLE 95% CI)
Imprinting protection (%)					
H1	66 (53, 77)	53 (32, 69)	64 (47, 77)	50 (23, 70)	54 (32, 70)
H3	33 (17, 46)	42 (24, 56)	34 (18, 47)	41 (22, 55)	41 (22, 56)
N2	0 (0, 7)	0 (0, 11)	0 (0, 8)	0 (0, 10)	0 (0, 11)
Age-specific risk of medically attended influenza A infection					
0-4 years	3.0 (2.5, 3.6)	N.A.	3.0 (2.5, 3.6)	N.A.	N.A.
5-9 years	2.6 (2.2, 3.0)	N.A.	2.5 (2.2, 3.0)	N.A.	N.A.
10-14 years	1.7 (1.4, 2.0)	1.8 (1.5, 2.1)	1.7 (1.4, 2.0)	1.8 (1.5, 2.1)	1.8 (1.5, 2.1)
15-19 years	1.2 (1.0, 1.5)	1.3 (1.0, 1.5)	1.2 (1.0, 1.5)	1.3 (1.0, 1.5)	1.3 (1.1, 1.6)
30-39 years	1.1 (0.9, 1.3)	1.1 (0.9, 1.3)	1.1 (0.9, 1.3)	1.1 (0.9, 1.3)	1.1 (0.9, 1.3)
40-49 years	0.9 (0.7, 1.1)	0.9 (0.8, 1.1)	0.9 (0.7, 1.1)	0.9 (0.8, 1.1)	0.9 (0.8, 1.1)
50-64 years	1.0 (0.8, 1.3)	0.9 (0.8, 1.2)	1.0 (0.8, 1.3)	1.0 (0.8, 1.2)	0.9 (0.8, 1.1)
65+ years	1.6 (1.2, 2.1)	1.4 (1.0, 1.8)	N.A.	N.A.	1.5 (1.1, 1.9)

Appendix 1 Table 2. Estimates of age-specific VE parameters in models fitted to different age groups.

	Model with age-specific VE, age \geq 6 months (MLE 95% CI)	Model with age-specific VE, age \geq 10 years (MLE, 95% CI)	Model with age-specific VE, age $<$65 years (MLE, 95% CI)	Model with age-specific VE, age 10-64 years (MLE, 95% CI)
Age-specific VE against H1N1 (%)				
0-4 years	69 (56, 84)	N.A.	68 (55, 83)	N.A.
5-9 years	26 (0, 48)	N.A.	24 (0, 47)	N.A.
10-14 years	92 (80, 96)	94 (82, 98)	92 (80, 96)	93 (81, 97)
15-19 years	86 (62, 95)	87 (64, 95)	86 (61, 95)	86 (62, 95)
20-29 years	84 (65, 91)	84 (65, 91)	83 (63, 90)	83 (64, 90)
30-39 years	8 (0, 37)	12 (0, 40)	5 (0, 35)	8 (0, 38)
40-49 years	18 (0, 45)	19 (0, 46)	14 (0, 42)	15 (0, 43)
50-64 years	32 (7, 51)	30 (4, 50)	28 (2, 48)	27 (0, 48)
65+ years	50 (16, 71)	56 (25, 75)	N.A.	N.A.
Age-specific VE against H3N2 (%)				
0-4 years	58 (48, 67)	N.A.	58 (48, 67)	N.A.
5-9 years	45 (31, 58)	N.A.	45 (30, 57)	N.A.
10-14 years	23 (0, 41)	26 (3, 45)	22 (0, 41)	25 (2, 44)
15-19 years	31 (3, 53)	35 (8, 56)	30 (2, 53)	34 (6, 55)
20-29 years	34 (11, 51)	37 (16, 53)	33 (11, 51)	36 (15, 53)
30-39 years	10 (0, 31)	15 (0, 35)	9 (0, 30)	14 (0, 34)
40-49 years	36 (15, 52)	42 (23, 57)	36 (15, 52)	42 (23, 57)
50-64 years	47 (35, 56)	50 (38, 59)	47 (35, 57)	49 (38, 59)
65+ years	41 (24, 54)	39 (22, 53)	N.A.	N.A.

Appendix 1 Table 3. Estimates of imprinting protection for models with different age groups.

Age groups (years)	Best-fitting model	H1 imprinting protection (% 95% CI)	H3 imprinting protection (% 95% CI)
0-4, 5-17, 18-64, 65+	Demography, age, HA imprinting, age-specific VE	56 (40, 68)	36 (25, 46)
0-8, 9-17, 18-49, 50-64, 65+	Demography, age, HA imprinting, age-specific VE	62 (47, 74)	35 (21, 48)

Appendix 1 Table 4. Estimates for VE from model with birth-cohort-specific VE fitted to people ≥ 10 years old.

Birth cohort	H1N1 VE (% MLE, 95% CI)	H3N2 VE (% MLE, 95% CI)
2003-2006	100 (70, 100)	7 (0, 41)
1998-2002	93 (80, 97)	29 (6, 47)
1988-1997	88 (75, 92)	54 (38, 67)
1978-1987	54 (26, 75)	16 (0, 34)
1968-1977	14 (0, 41)	25 (2, 43)
1953-1967	19 (0, 40)	44 (32, 54)
1918-1952	52 (24, 71)	45 (33, 55)

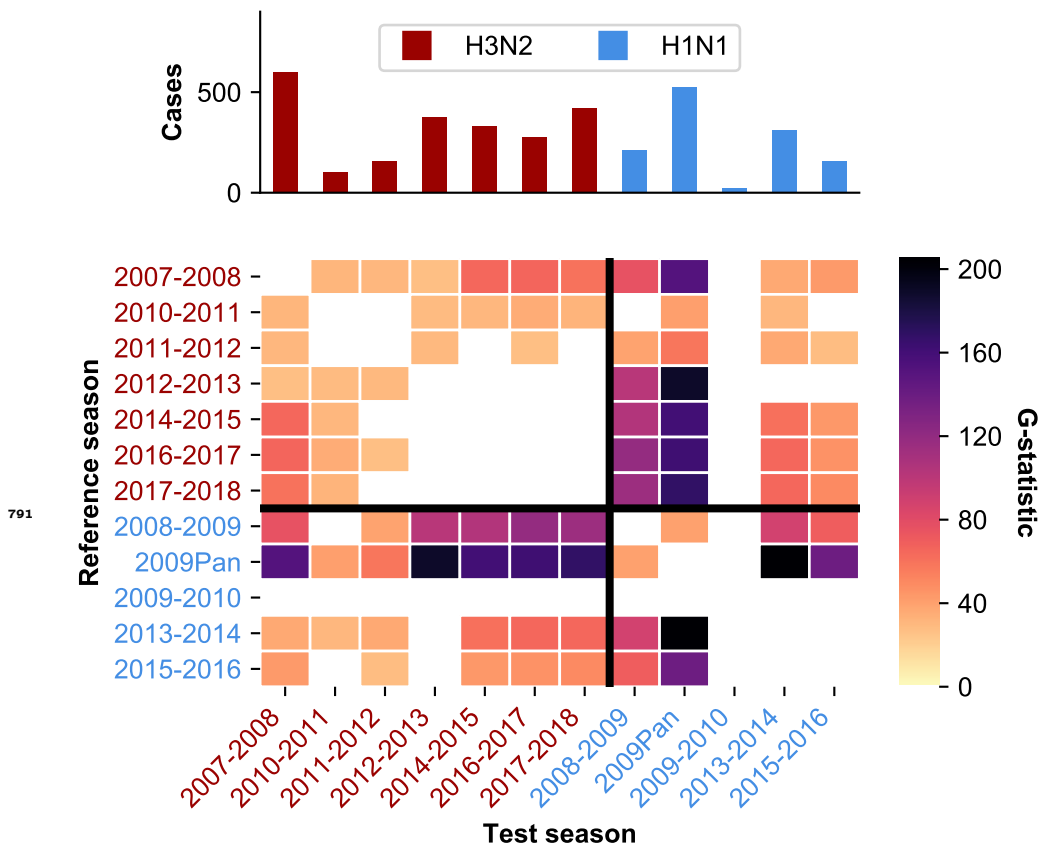


Figure 1-Supplement 1. Seasons differ significantly in their age distributions. Colored cells indicate that two seasons have significantly different age distributions (Bonferroni-corrected $p < 0.05$), and color intensity shows the observed G-test statistic (Materials and Methods: "Calculating differences in the age distribution between seasons."). White cells denote seasons that did not have significantly different age distributions from each other. The dominant subtype of each season is indicated by the label color.

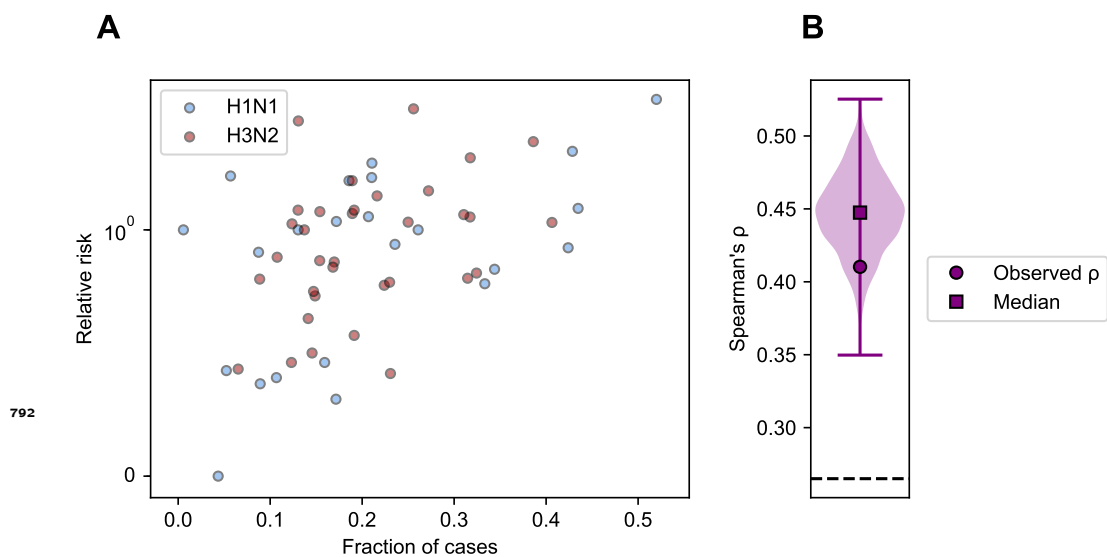


Figure 1-Supplement 2. **A.** Each point shows an age group's relative risk of infection during the first half compared to the second half of an epidemic period (y-axis) and the fraction of cases belonging to that age group (x-axis) (Materials and Methods: "Calculating relative risk"). Points are colored by the dominant subtype of the season. **B.** To account for potential undersampling of cases at the beginning and end of specific seasons, we simulated 1000 replicate epidemics (Materials and Methods: "Sensitivity to sampling effort") and calculated the same correlation as in panel **A**. The range is indicated by a vertical line and the median by a square. Horizontal dashed black line indicates the critical value of ρ below which the correlation is not significant.

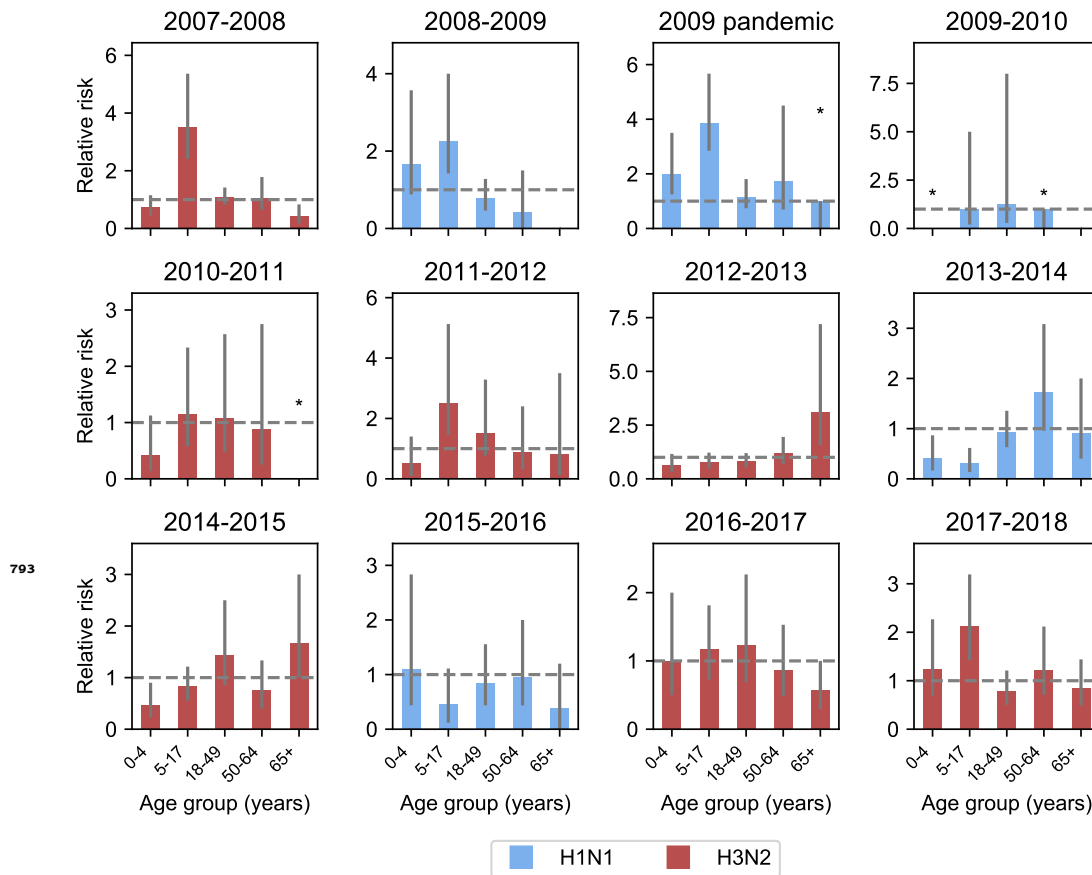


Figure 1-Supplement 3. Each panel shows the relative risk of infection in the first versus the second half of an epidemic for different age groups in each season (Materials and Methods: "Calculating relative risk"). Relative risk greater than 1 (indicated by the grey dashed line) means that an age group was more likely to be infected at during the first rather than second half of an epidemic. Age groups with no cases in the latter half of a season are indicated by asterisks and no bar. The dominant subtype of each subtype is indicated by the bar color. 95% binomial confidence intervals are indicated by grey vertical lines. Bars with asterisks over them indicate that the 95% confidence interval includes the scenario where all cases occur in the first half of the season.

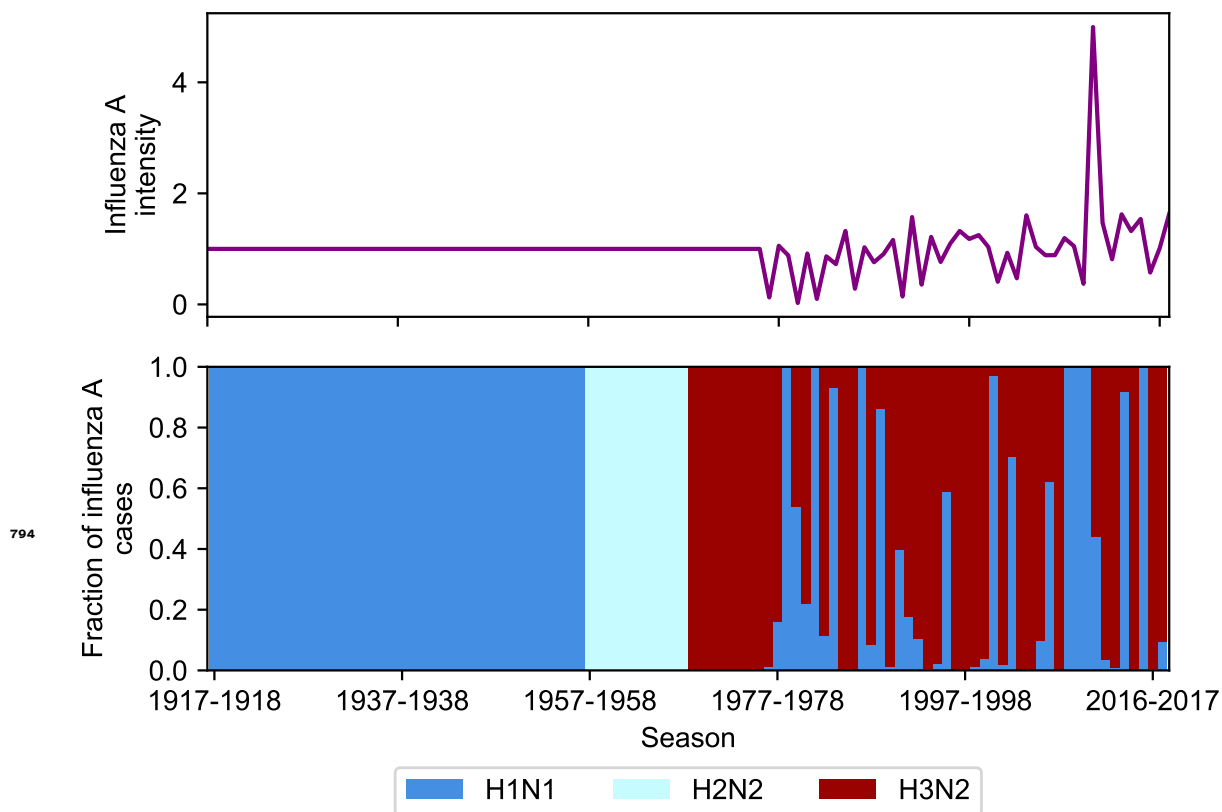


Figure 2-Supplement 1. The intensity (top panel) and subtype frequencies (bottom panel) of influenza A seasons in the United States. Intensity is measured as the product of influenza-like illness (ILI) and the fraction of respiratory specimens testing positive for influenza A in national surveillance data (Materials and Methods: "Seasonal intensity"). This is normalized to the average intensity value between 1977 and 2017-2018. Seasons before 1977 where United States ILI surveillance data are unavailable are assumed to have an intensity score of 1 (i.e., the average score over all other seasons). Subtype frequencies were obtained from national surveillance data before the 2007-2008 season and directly from the Marshfield studies afterwards.

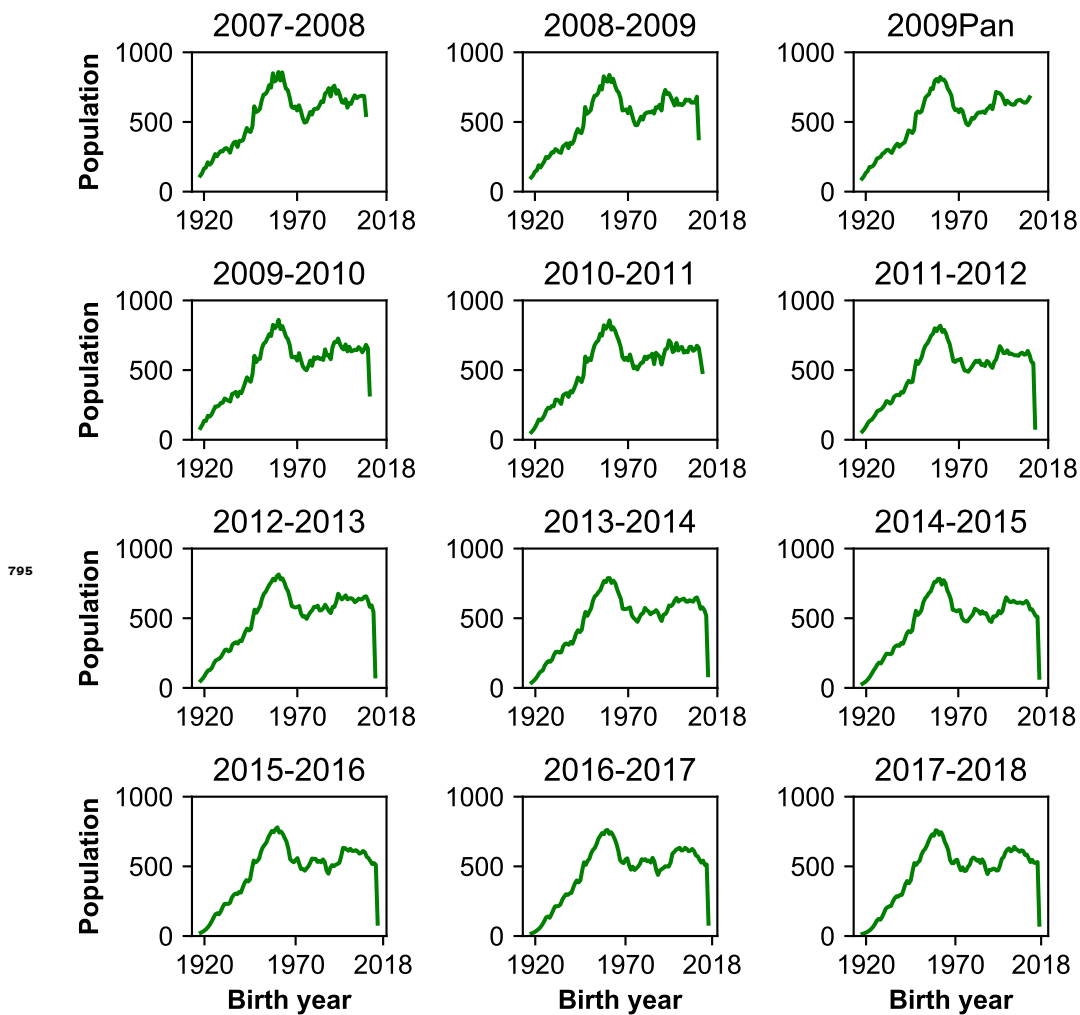


Figure 3-Supplement 1. Each panel shows the population distribution of all individuals in the study area who met the age criteria for study enrollment. People under 6 months old at the start of the sampling period in a season were not eligible to participate.

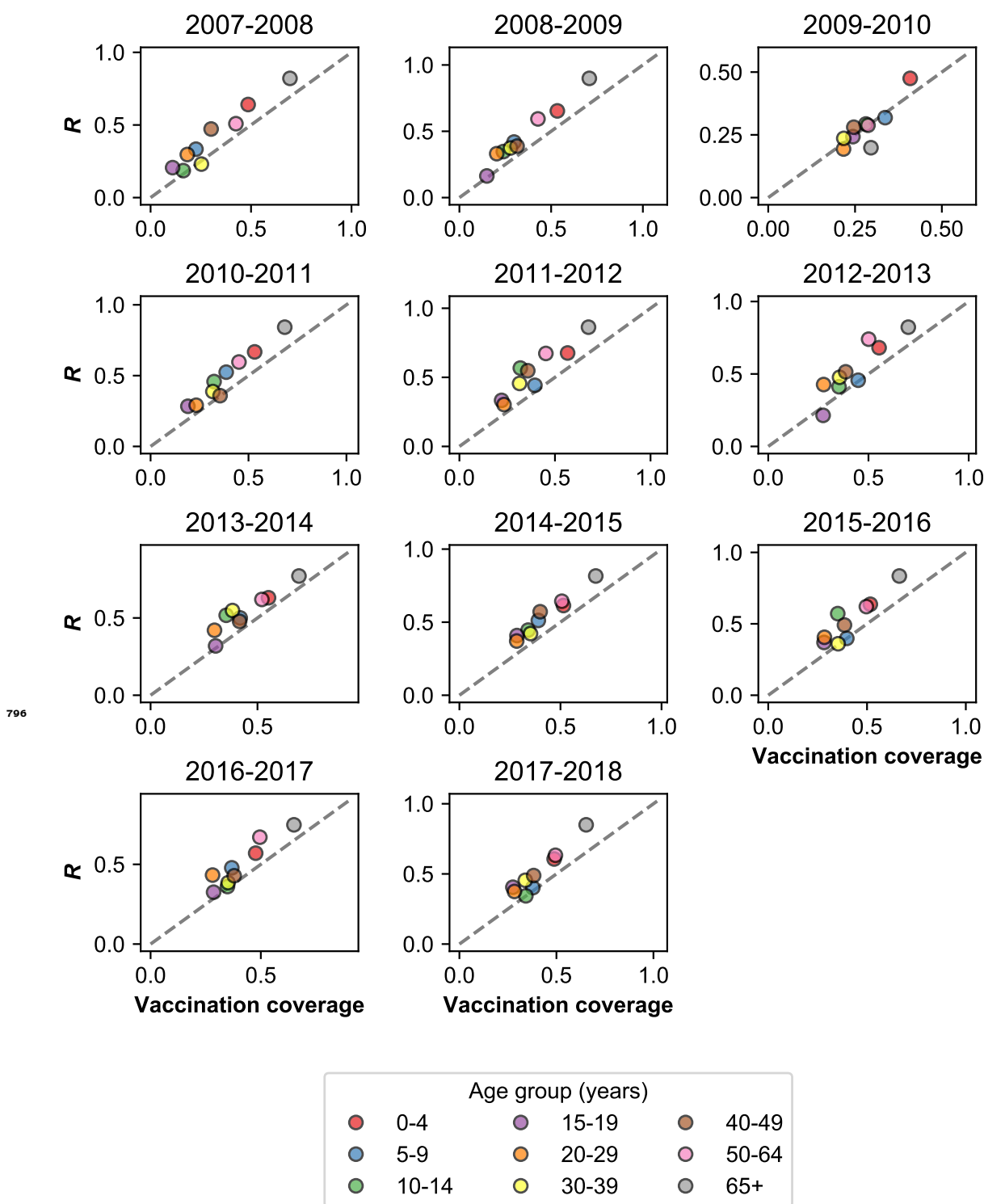


Figure 3-Supplement 2. Vaccinated individuals seek healthcare for MAARI at a higher rate than predicted by vaccination coverage. We measured the fraction of vaccinated people among all who presented with MAARI and tested negative for influenza ($R = \frac{\text{Vaccinated test-negative controls}}{\text{Unvaccinated test-negative controls} + \text{Vaccinated test-negative controls}}$, Materials and Methods: "Vaccination"). This is plotted against vaccination coverage by season for different age groups. The dashed grey line shows where R and vaccination coverage are equal. Vaccination coverage for the 2009-2010 season uses monovalent vaccination coverage estimated directly from all individuals with MAARI. We do not show the 2009 pandemic season because the monovalent vaccine was not distributed until the second wave of the pandemic.

797

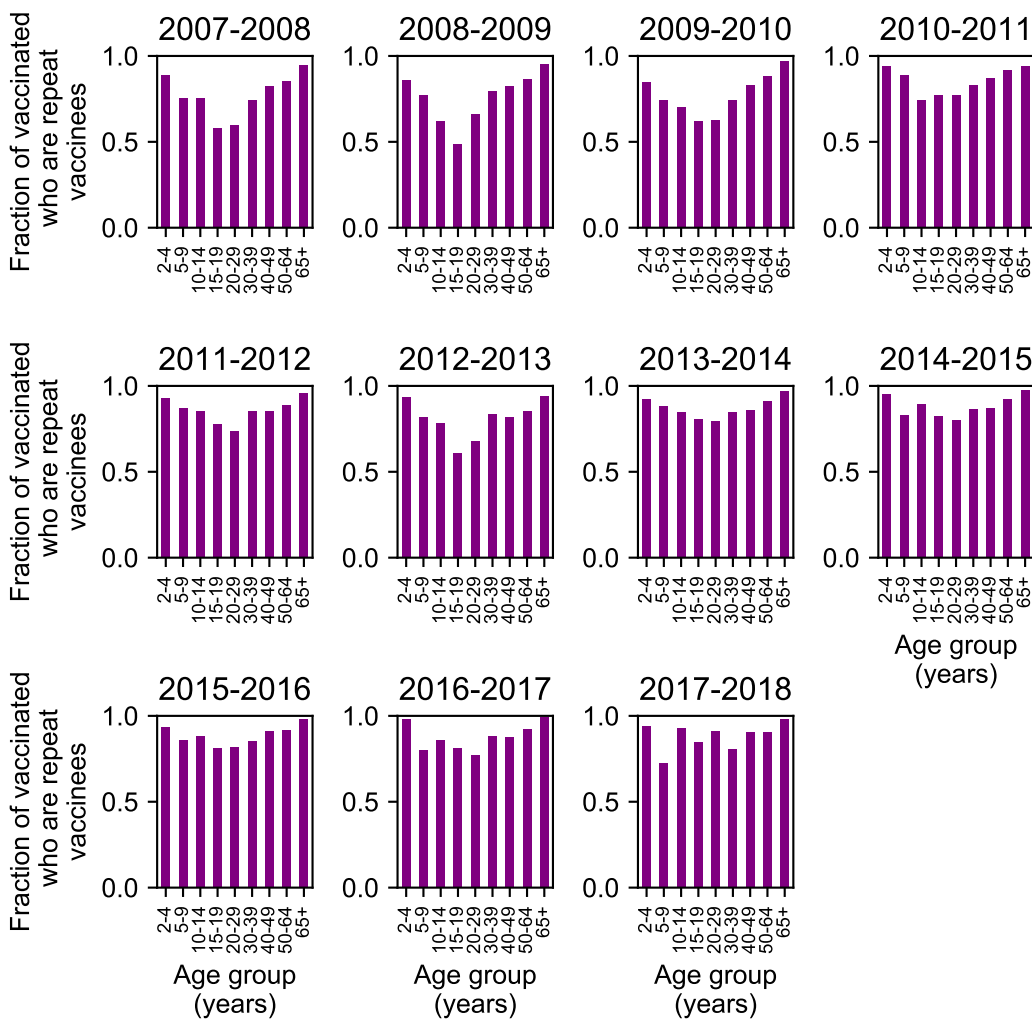


Figure 3-Supplement 3. Repeat vaccination varies by age group and season. Each bar shows the fraction of individuals who were vaccinated in that season who also received at least one influenza vaccination in the previous two seasons.

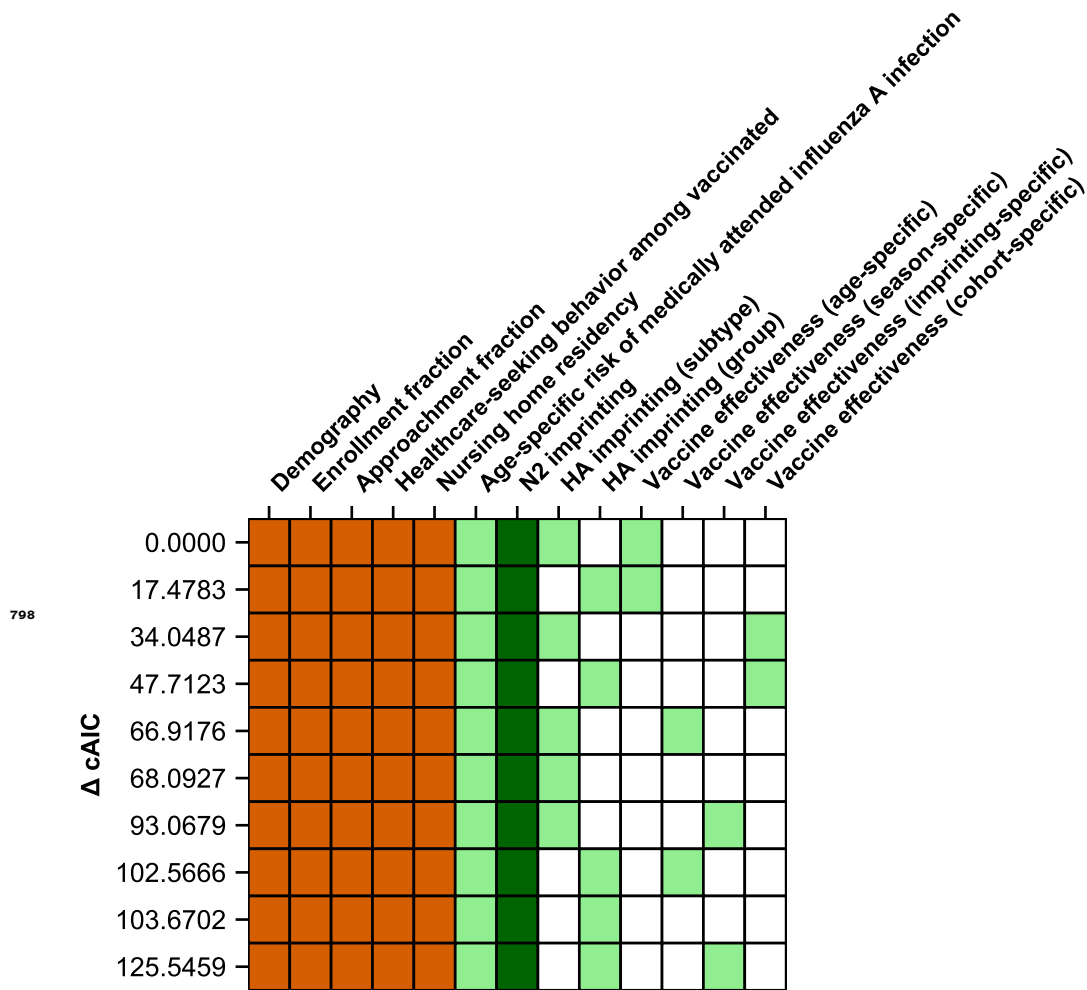
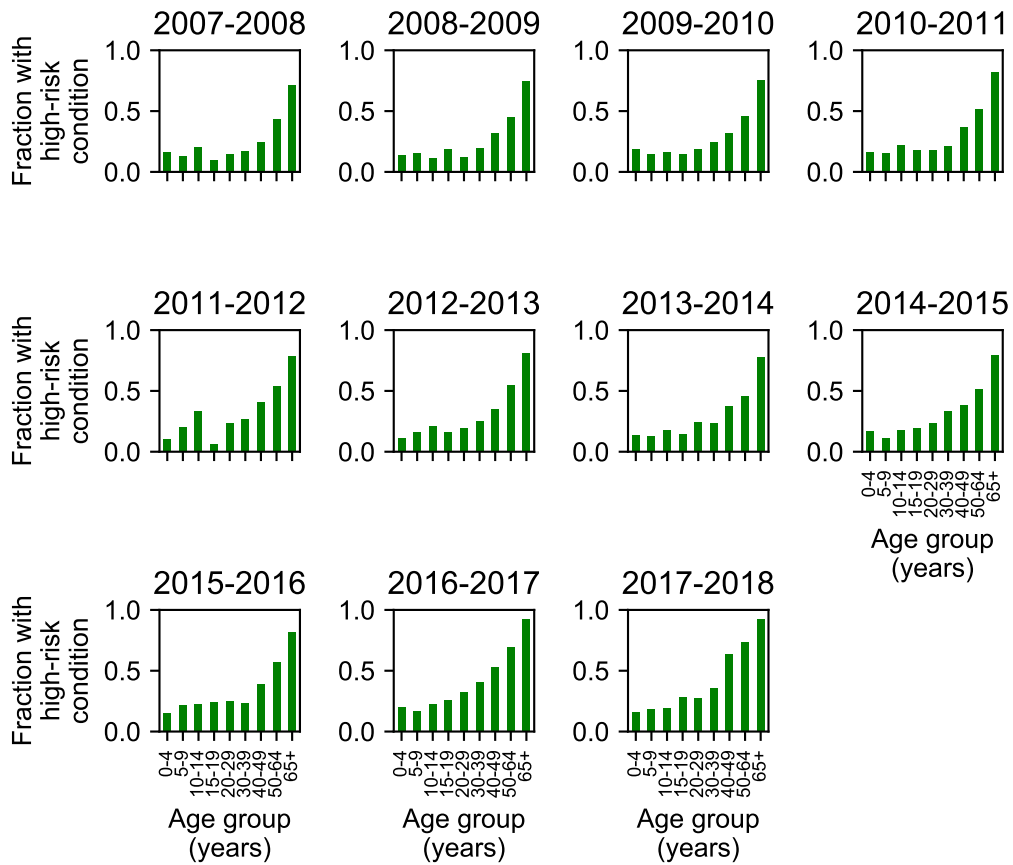


Figure 4-Supplement 1. The best-fitting model includes age-specific risk of medically attended influenza A infection, HA subtype imprinting, and age-specific VE. The ten main models are shown as rows with colored squares indicating whether that model included parameters indicated by the columns. Orange squares indicate covariates that were not estimated. Light green squares mean that a given estimated parameter was supported. Dark green squares mean that the model did not support the inclusion of the parameters indicated by the column (i.e., the CI includes 0). Models are sorted by their cAIC relative to the best-fitting model.



799

Figure 4-Supplement 2. High-risk medical status varies with age but stays relatively consistent across seasons. Each plot shows the fraction of enrolled people who had a high-risk medical condition for each season. High-risk medical condition data was not collected for the 2009 pandemic season.

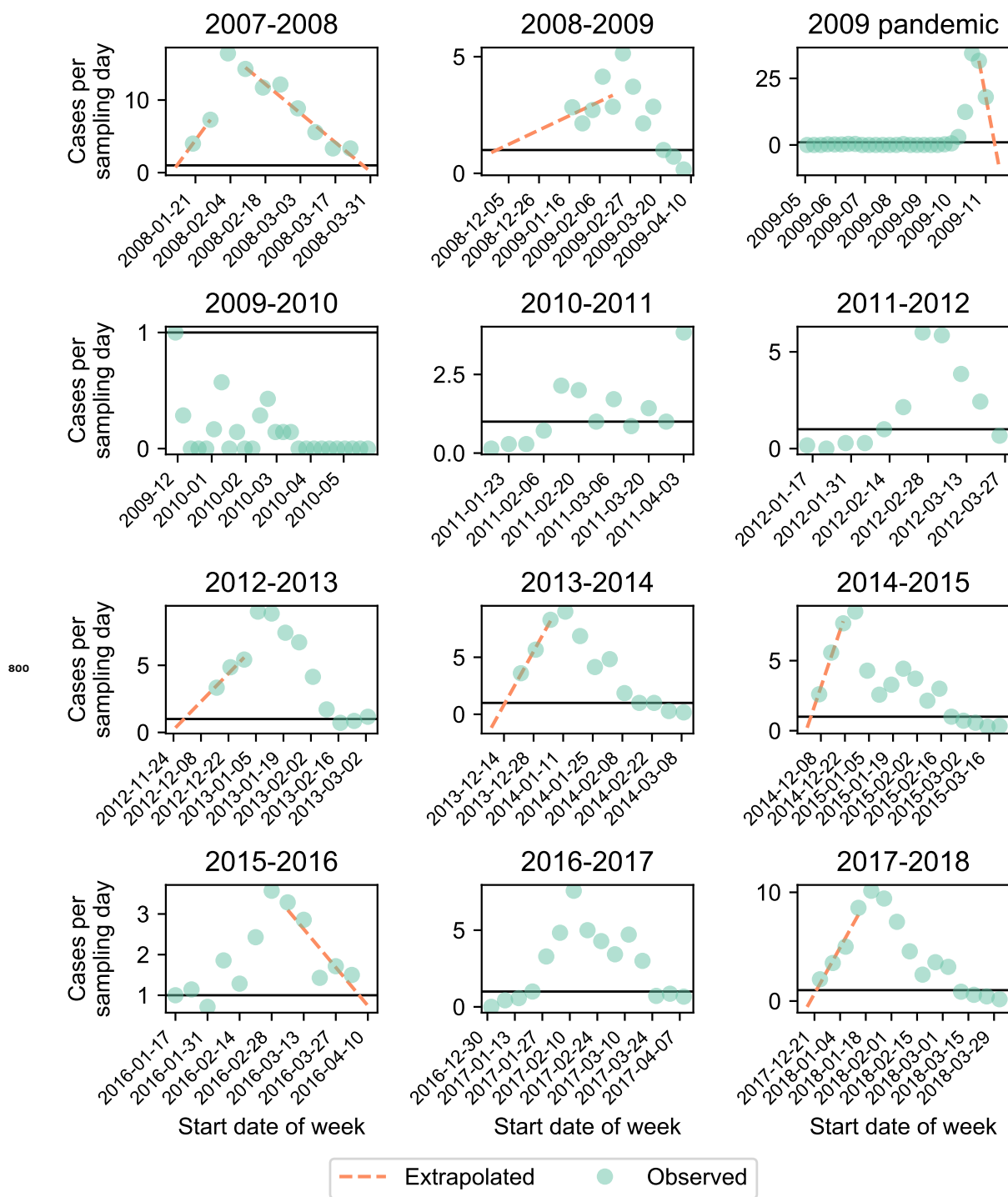


Figure 5-Supplement 1. The starts and ends of some seasons were undersampled. Each panel shows the number of cases per sampling day (green circles). We extrapolated cases at the start and end of the season (orange dashed line) if the observed number of cases per day exceeded 1 (black line) at the start and end of that season (Materials and Methods: "Sensitivity to sampling effort").

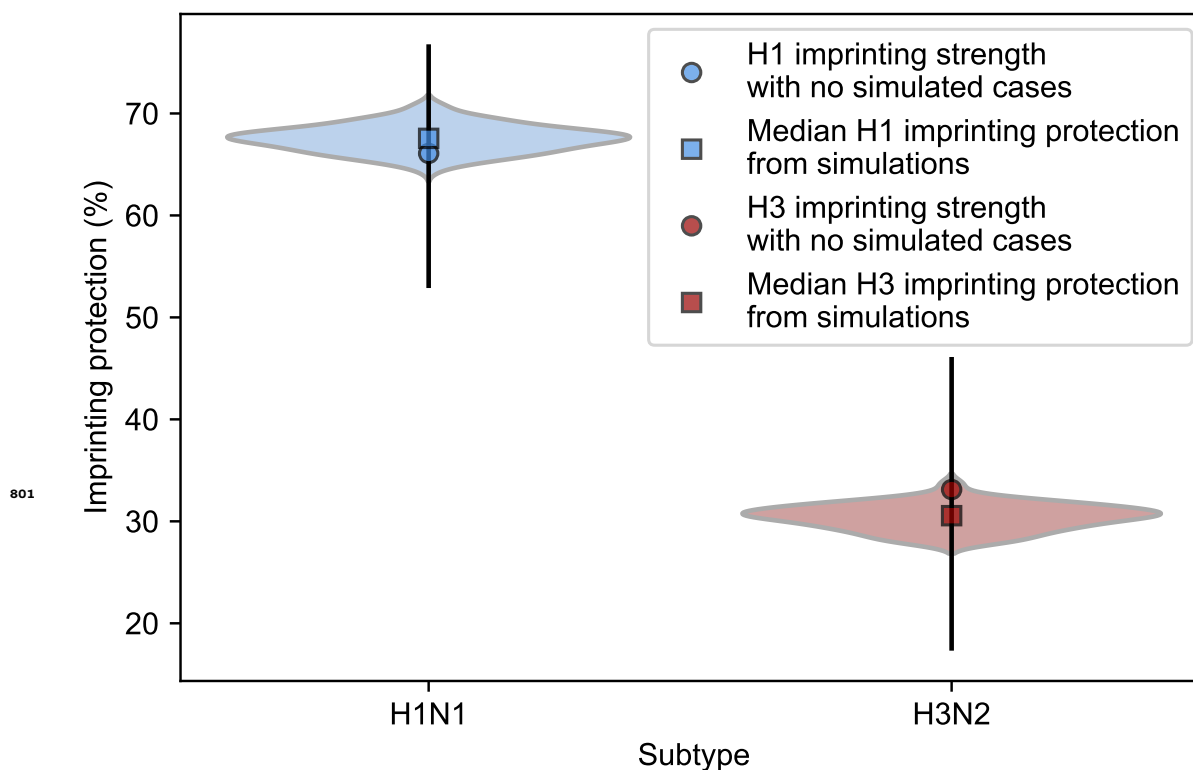


Figure 5–Supplement 2. The strength of imprinting protection does not change significantly after correction for unequal sampling between seasons. We fitted the model to simulated cases in seasons where the enrollment period does not fully overlap the epidemic period and recorded the maximum likelihood estimates for H1N1 and H3N2 imprinting protection (Materials and Methods: "Sensitivity to sampling effort"). The distributions of these values are shown as violin plots and the medians are shown as squares. Estimates of imprinting protection from the best fitting model without simulated data with a 95% confidence interval are shown as circles with error bars.

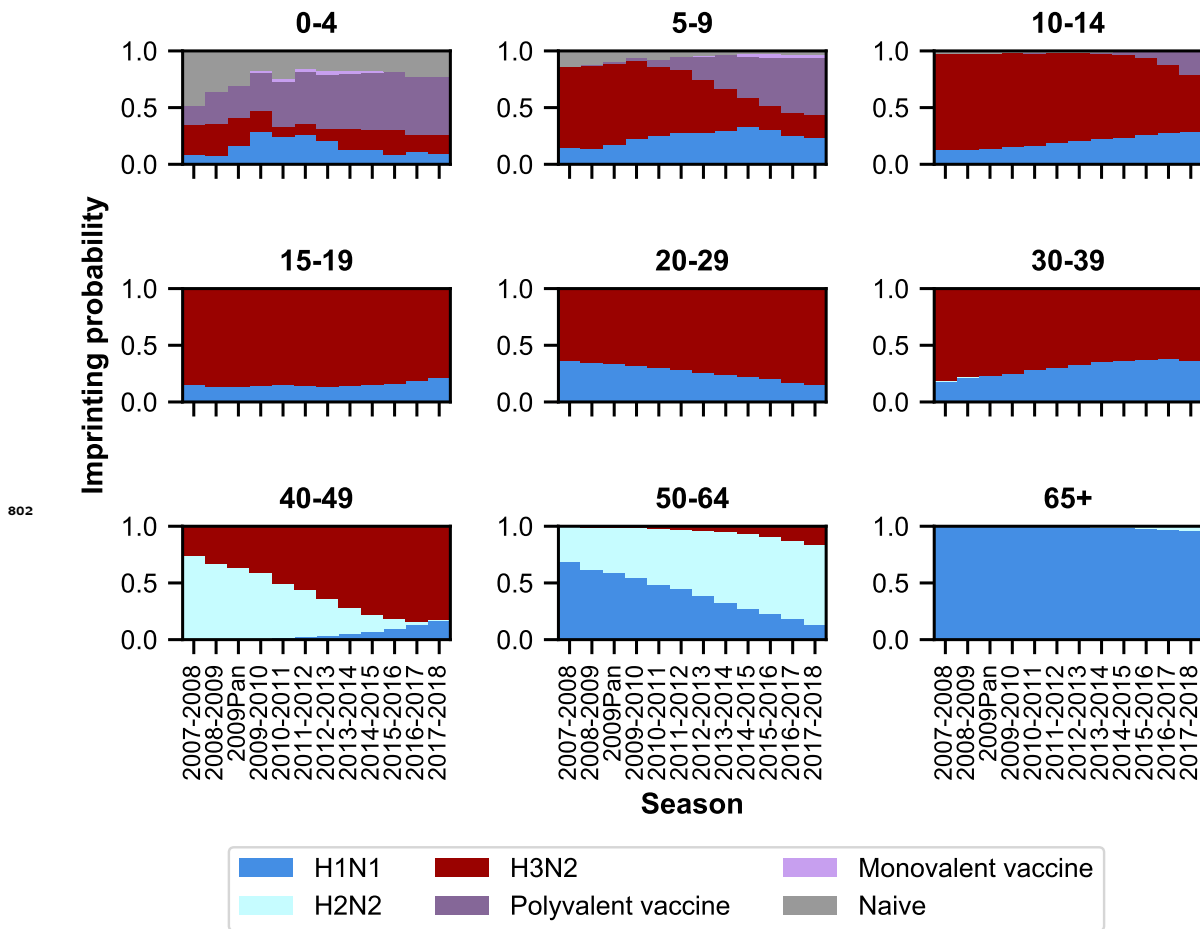
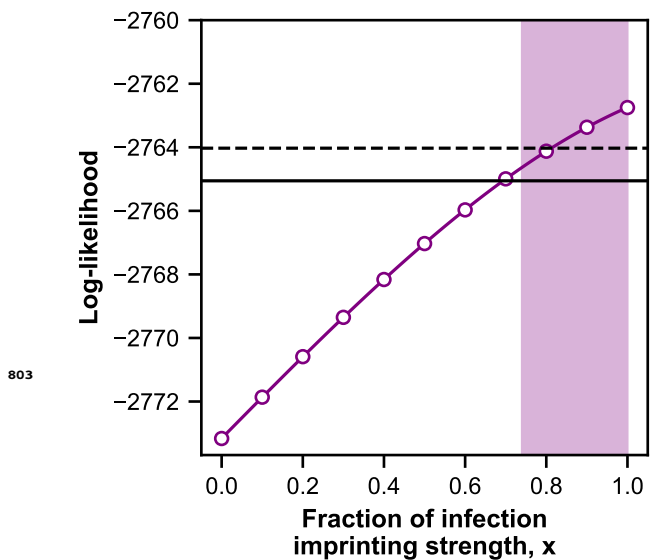
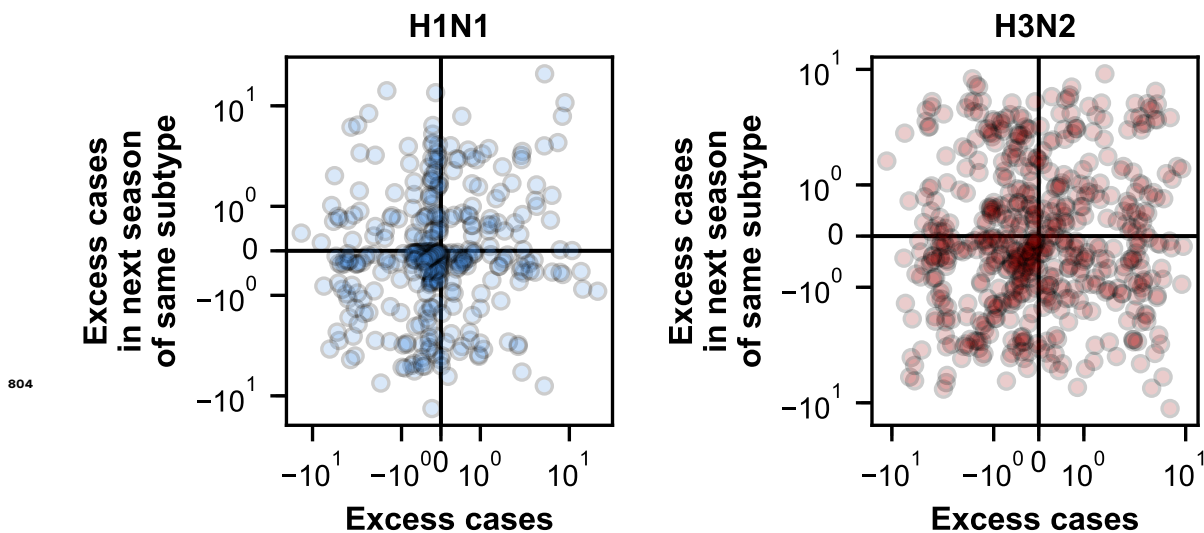


Figure 5-Supplement 3. Each panel shows the imprinting probabilities for a specific age group from the 2007-2008 season through the 2017-2018 season, including vaccination as a potential first exposure.



803

Figure 5-Supplement 4. Vaccine imprinting improves model fit. Plot shows the likelihood profile of the parameter x , which describes the strength of protection from initial exposure via vaccination as a fraction of the protection conferred by initial infection (Materials and Methods: "Vaccine imprinting"). The solid black line shows the log-likelihood of the best-fitting model without protection from vaccine imprinting, and the dashed line shows the log-likelihood threshold for a $\Delta cAIC$ of 0 compared to the best fitting model with the addition of one free parameter (i.e., x). Shaded area shows 95% CI for x .



804

Figure 5-Supplement 5. Excess cases in a season are weakly correlated with excess cases in the next season with the same dominant subtype. We tested whether excess cases in each birth cohort were negatively correlated with excess cases in the same birth cohort in the next season of the same subtype (Materials and Methods: "Calculating excess cases"). If the protective effects of recent infection are not captured in our model, we expect that an excess of cases in one season should lead to a depletion in cases in the next season (i.e., negative correlation). We instead find a weak positive correlation for cases of H1N1 (Spearman's $\rho=0.12$, $p=0.02$) and H3N2 (Spearman's $\rho=0.05$, $p=0.19$).

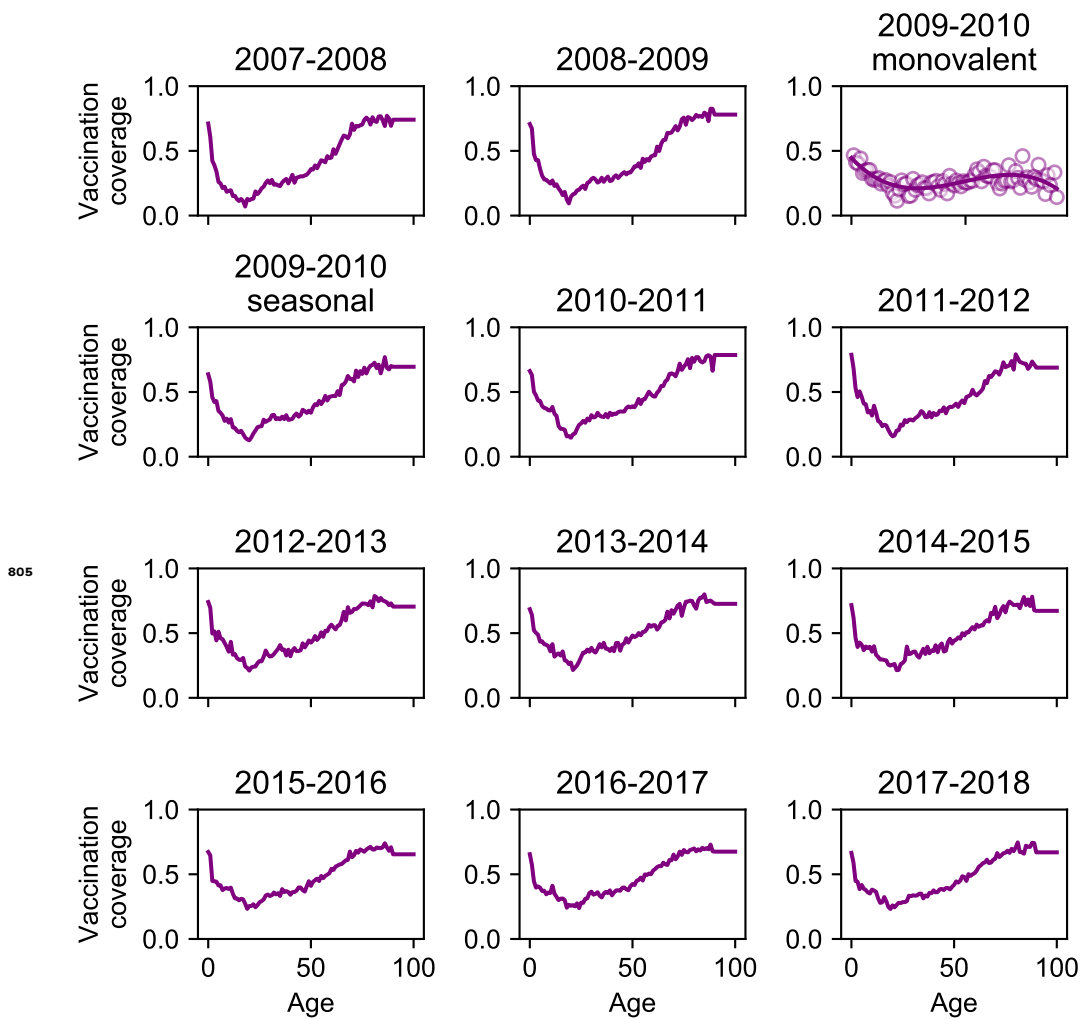


Figure 5–Supplement 6. Vaccination coverage in the Marshfield Epidemiological Study Area for seasons 2007-2008 through 2017-2018. We estimated monovalent vaccination coverage in 2009-2010 by measuring vaccination coverage among enrolled people and fitting a smoothing spline to the data (solid line).

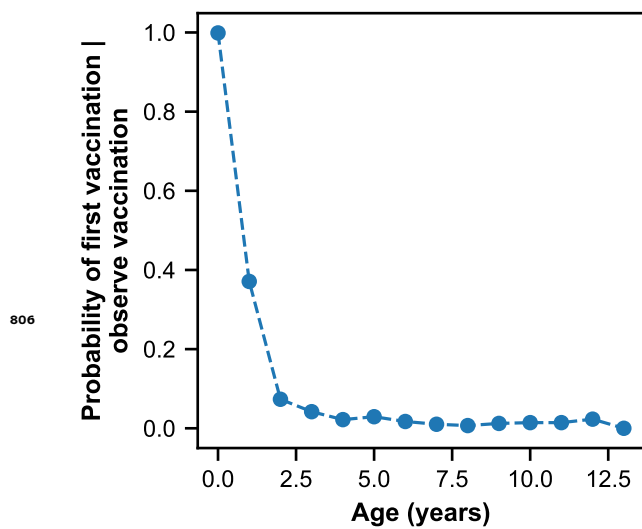


Figure 5–Supplement 7. The probability of an individual receiving their first vaccination declines with age. Each point represents the fraction of people enrolled in the Marshfield study who received their first vaccination among all vaccinated individuals of that age.

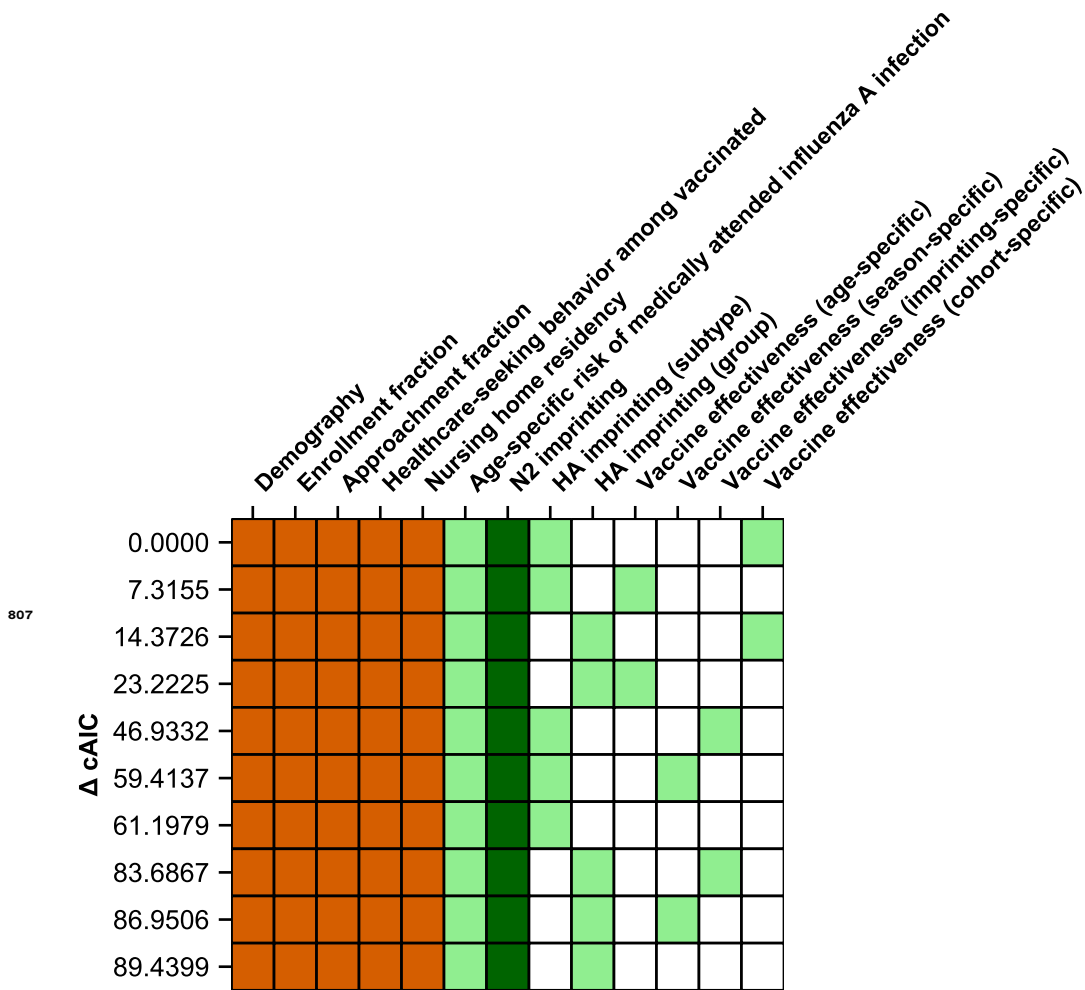


Figure 6-Supplement 1. A model including age-specific risk of medically attended influenza A infection, HA subtype imprinting, and birth-cohort-specific VE best fits cases of people ≥ 10 years old. The ten main models are shown as rows with colored squares indicating whether that model uses parameters indicated by the columns. Orange squares indicate covariates that were not estimated. Light green squares mean that a given estimated parameter was supported. Dark green squares mean that the model did not support the inclusion of the parameters indicated by the column (i.e., the CI includes 0). Models are sorted by their cAIC relative to the best-fitting model.

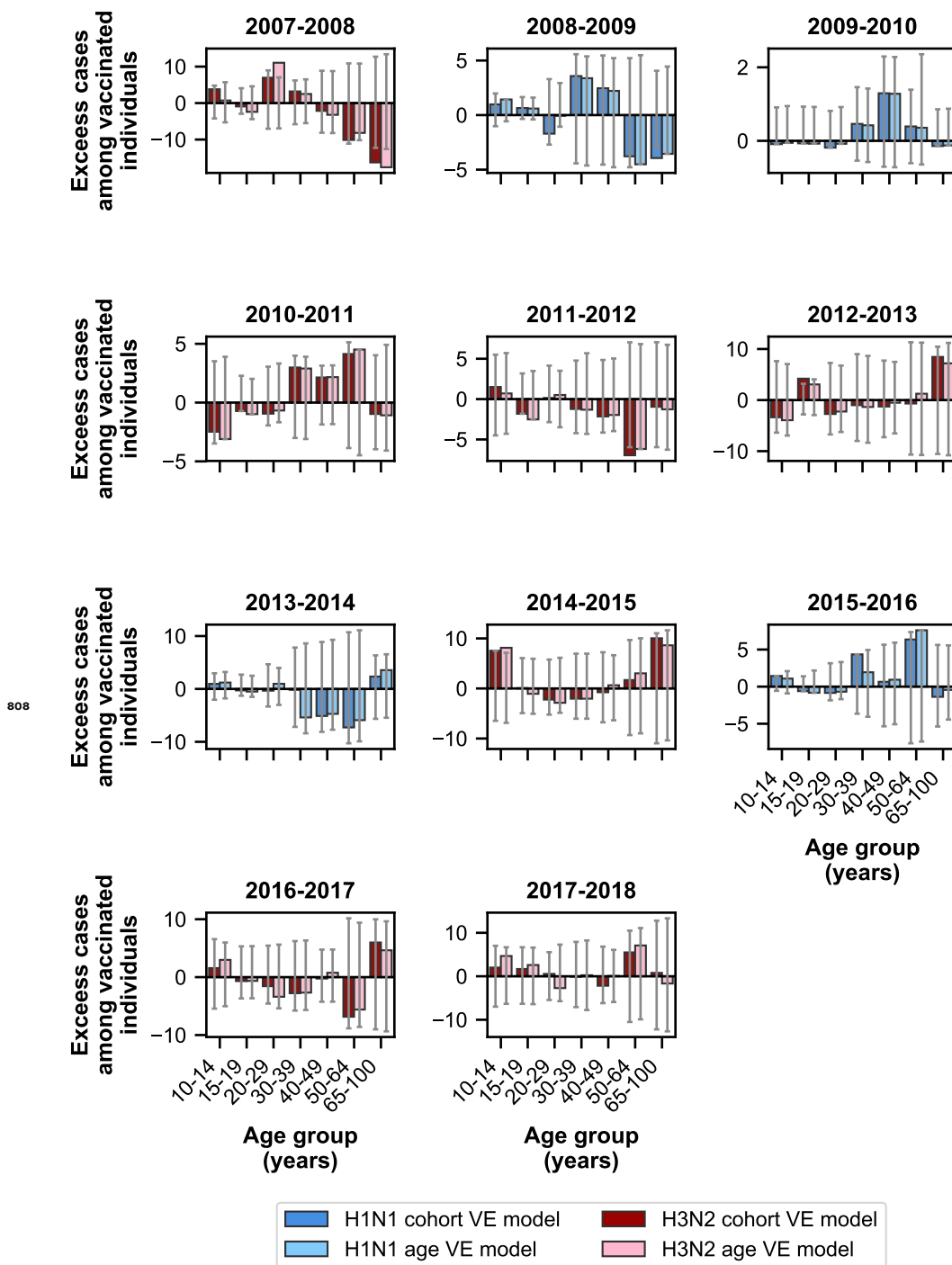


Figure 6-Supplement 2. The birth-cohort-specific VE model predicts observed cases better than the age-specific VE model for people ≥ 10 years old. Bars show the excess cases in vaccinated individuals relative to the birth-cohort-specific VE model (dark colors) and the age-specific VE model (light colors) for age groups ≥ 10 years old. Colors indicate the dominant subtype of a given season. 95% prediction intervals are shown as grey error bars.